

MMS Project

Long-Term Integrity of Deepwater Cement Systems Under Stress/Compaction Conditions

Report 4

Issued April 10, 2003



CEMENTING SOLUTIONS, INC.



Table of Contents

Objectives	1
Observations and Recommendations for Future Work	1
Testing Program and Procedures	2
<i>Cement Design Performance Testing</i>	<i>3</i>
<i>Mechanical Properties Testing</i>	<i>3</i>
<i>Mechanical Integrity Testing</i>	<i>4</i>
<i>Numerical Simulation</i>	<i>4</i>
<i>New Testing Methods</i>	<i>4</i>
Shear Bond and Annular Seal Test Modifications	4
Cement Column Seal Tests	5
Hydrostatic Testing to Anelastic Strain and Fatigue	5
Test Results	5
<i>Tensile Strength</i>	<i>5</i>
<i>Young's Modulus with Various Confining Forces</i>	<i>6</i>
<i>Poisson's Ratio Testing</i>	<i>6</i>
<i>Strain Tests</i>	<i>7</i>
<i>Rock Properties Testing</i>	<i>7</i>
<i>Shear Bond Tests</i>	<i>10</i>
<i>Annular Seal Tests</i>	<i>10</i>
Appendix A—Test Procedures	11
<i>Modified Blending Procedures</i>	<i>11</i>
<i>Free-Fluid Testing</i>	<i>11</i>
<i>Compressive Strength Testing</i>	<i>12</i>
Sample Curing	12
<i>Young's Modulus and Poisson's Ratio Testing</i>	<i>12</i>
<i>Anelastic Strain and Cycling</i>	<i>13</i>
<i>Tensile Strength and Tensile Young's Modulus</i>	<i>13</i>



<i>Annular Seal Testing Procedure</i>	14
Simulated Soft-Formation Test.....	14
Simulated Hard-Formation Test	15
Simulated Moderate-Strength Formation Test	15
Temperature and Pressure Cycling.....	15
<i>Shear Bond Strength Testing</i>	16
Pressure Cycling Schedule	17
Temperature Cycling Schedule	17
<i>Cement Column Seal Tests</i>	18
Appendix B—Test Data	20
Appendix C—Numerical Modeling	35
<i>Introduction</i>	35
<i>Mathematical Model</i>	36
Assumptions	38
Stress Conditions	38
Parametric Studies	39



Objectives

The overall objective of this project is to determine the properties that affect cement's capability to produce a fluid-tight seal in an annulus. The project primarily focuses on deepwater applications, but general applications will also be examined. The research conducted thus far is focused on the measurement of cement's mechanical properties and correlation of these properties to the cement's performance. Also, research was conducted to determine which laboratory methods should be used to establish the cement's key properties.

Results obtained during this reporting period focused on

- continued measurement of mechanical properties of tensile strength and Young's modulus under various confining loads
- mechanical bond integrity testing to include shear bond and annular seal testing on specimens cured under various cyclic curing schedules
- mathematical simulation of stresses induced in a cemented annulus

These results are tabulated in the Results section below. All rock properties test results developed during this project, including available graphical data, are presented in Appendix B.

Observations and Recommendations for Future Work

Results of testing during this reporting period indicate:

1. Significant variation in Poisson's ratio with varying stress rate. Loading samples at a faster rate resulted in higher Poisson's ratio values. Inclusion of a CT scan for mechanical properties samples revealed another variable: air entrainment. The presence of entrained air appeared to lower Poisson's ratio values.
2. Questions regarding comparability of data for different compositions normalized with respect to each composition's hydrostatic yield strength. A modification of the test procedure is suggested to standardize the confining stress at 500-psi and cycle samples repeatedly to 25%, 50%, and 75% of each composition's compressive strength under that confining stress. Measurement of anelastic strain with cycling should provide a more comparable value of each composition's performance.
3. Several compositions tested in the annular seal apparatus did not fail with repeated cycling. Therefore, the addition of more aggressive test conditions is required to induce seal failure. The addition of an intermediate formation strength is also proposed for further quantifying the performance of various compositions.

Future work includes:

- implementation of a modified test procedure with future testing
- quantification of anelastic strain magnitudes and analysis of consequences in the well environment



- completion of numerical analyses after annular seal testing is complete

Testing Program and Procedures

This section does not flow as well as it could. I assume that the Task 1 is completed; are these tasks performed sequentially or concurrently?

The following cement slurries will be examined: Type 1 cement, foamed cement, bead cement, Class H cement, and latex cement. The effects of fibers and expansion additives on the performance of various cements are also examined. The cements are tested primarily for deepwater applications, but their performance under all application conditions is also examined.

Tasks in the project are listed below:

- Task 1 – Problem Analysis
- Task 2 – Property Determination
- Task 3 – Mathematical Analysis
- Task 4 – Testing Baseline
- Task 5 – Refine Procedures
- Task 6 – Composition Matrix
- Task 7 – Conduct Tests
- Task 8 – Analysis of Results
- Task 9 – Decision Matrix

Compositions tested in this project are outlined in Table 1 below. The compositions chosen represent those that are traditionally used in deepwater applications as well as newly developed compositions and compositions designed to improve performance.

**Table 1—Cement Compositions for Testing**

Description	Cement	Additives	Water Requirement (gal/sk)	Density (lb/gal)	Yield (ft³/sk)
Neat Type I slurry	Type 1	—	5.23	15.6	1.18
Type I slurry with fibers	Type 1	3.5% carbon fibers-milled	5.2	15.6	1.16
Latex slurry	Type 1	1.0 gal/sk LT-D500	4.2	15.63	1.17
Latex slurry with fibers	Type 1	1.0 gal/sk LT-D500 3.5% carbon fibers-milled 0.50% Melkcrete	4.09	15.63	1.20
Foam slurry (12-lb/gal)	Type 1	0.03 gal/sk Witcolate 0.01 gal/sk Aromox C-12 1% CaCl	5.2	12.0	1.19
Bead slurry	Type 1	13.19% K-46 beads	6.69	12.0	1.81
Neat Class H slurry	Class H	—	4.3	16.4	1.08
Class H slurry with fibers	Class H	—	4.3	16.4	1.08
Sodium metasilicate slurry	Type 1	—	14.22	12.0	2.40

Testing and analysis of the cements is divided into four categories:

1. cement design performance testing
2. mechanical properties testing
3. mechanical integrity testing
4. numerical simulation

Cement Design Performance Testing

Standard cement design performance testing, including rheology, thickening time, free fluid, set time, compressive strength, etc. are performed according to procedures outlined in API Spec. 10.

Mechanical Properties Testing

Mechanical properties tested include: tensile strength/tensile Young's modulus (T), compressive Young's modulus, Poisson's ratio, and hydrostatic pressure cycling.

Tensile strengths are determined with the Brazilian Test Method. From this test, the tensile Young's modulus (T) will be computed, as well as the maximum yield of the slurry.

The compressive Young's modulus are determined through compression tests with confining loads (defined by 0-psi break) with a baseline of a 14-day cure. Chandler's new



mechanical properties device will also obtain acoustic data on the slurry used in these tests. The Poisson's ratio will also be determined from these tests, and it is variable with respect to the stress rate, slurry type, presence of air entrainment, and perhaps other variables.

Mechanical Integrity Testing

The mechanical integrity issues of the cement slurries include the flow of fluids around the cement, through the matrix of the cement, and stresses in the cement. To predict the flow of fluid around the cement, various cement slurries will be tested for bonding capability, microannuli formation, and deformation. The flow of fluids through the matrix of the cement will be examined through tests of the cement slurries' resistance to cracking and permeability changes. The stress applied to the cement slurries will be determined as a function of pressure, temperature, pipe buckling, and formation compaction. The stresses will also be determined under cyclic conditions.

Shear bond and annular seal measurements are taken under cyclical conditions for both soft and hard formations. The cement specimens to be tested for shear bond are cured at 45°F for 14 days and then temperature-cycled once per day from 45°F to 180°F and back to 45°F during the cycling period.

The temperature cycling procedure is as follows:

1. Samples are placed in a 96°F water bath for 1 hour.
2. Samples are placed in a 180°F water bath for 4 hours.
3. Samples are placed in a 96°F water bath for 1 hour.
4. Samples are placed back into a 45°F water bath.

Numerical Simulation

Deepwater cement systems will be numerically modeled to aid in the understanding of how various stress conditions affect the long-term integrity of cement. This process is discussed in detail in Appendix C of this report.

New Testing Methods

Shear Bond and Annular Seal Test Modifications

Results from testing thus far with hard formation and soft formation simulation indicate the need for a simulated formation of intermediate strength. The altered shear and annular seal testing will include a simulated medium-strength formation with Schedule 40 PVC pipe as the outside mold for the cement sheath.

Additional stresses will be imposed on all test specimens by increasing the maximum pressure to which the inner pipe is stressed. Additionally, shear bond tests will be run only after a composition has been tested for annular seal. The shear bond test specimens



will be subjected to the same pressure cycling and temperature cycling that produced annular seal failure. This will provide a comparison between shear bond and annular seal behavior.

Cement Column Seal Tests

A series of cement column seal tests was initiated to illustrate the sealing effectiveness of several cements that are subjects of the project. These tests are designed to test a cement's ability to isolate gas pressure across an enclosed column. Ten-foot lengths of 2-in. pipe are filled with cement slurry, pressurized to 1000 psi, and then cured for eight days. After curing, low-pressure gas (100 or 200 psi) is periodically applied to one end of each test pipe and the gas flow rate through the cement column is measured. This testing will continue for the duration of the project.

Hydrostatic Testing to Anelastic Strain and Fatigue

Hydrostatic test results were reviewed, and questions were raised regarding comparability of data for different compositions normalized with respect to each composition's hydrostatic yield strength. The group decided to modify the test procedure to standardize confining stress at 500 psi and cycle samples repeatedly to 25%, 50%, and 75% of each composition's compressive strength under that confining stress. Measurement of anelastic strain with cycling should provide a more comparable value of each composition's performance.

Test Results

This section contains results from testing conducted throughout this project period, as well as results from previous test periods. All mechanical property test results and performance test results obtained throughout the project are tabulated here. Graphical data for all mechanical property tests are presented in Appendix B of this report.

Tensile Strength

The results of all tensile strength tests are presented in Tables 2 through 6. Table 2 illustrates the effects of carbon fibers on tensile strength. The two- to three-fold increase in tensile strength is significant, indicating the potential for fibers to increase the durability of cement.

Table 2—Tensile Strength and Young's Modulus

Slurry	Tensile Strength (psi)	Young's Modulus
Foam slurry (12-lb/gal)	253	3.23 E4
Neat Type I slurry	394/213	19.15/8.16 E4
Type I slurry with fibers	1071	9.6 E4
Latex slurry	539	5.32 E4
Latex slurry with fibers	902	8.5 E4



Young's Modulus with Various Confining Forces

The effects of confining stress on compressive strength and Young's modulus are presented in Tables 3 through 6. These results indicate a significant increase in compressive strength with increasing confining stress in lower-strength compositions such as foam cement and latex cement.

Table 3—Type I, Compressive Young's Modulus

Confining Pressure (psi)	Effective Strength (psi)	Young's Modulus (psi)
0	8645	16.7 E5
1500	8160	11.1 E5
5000	8900	9.1 E5

Table 4—12-lb/gal Foam, Compressive Young's Modulus

Confining Pressure (psi)	Effective Strength (psi)	Young's Modulus (psi)
0	2885	5.8 E5
500	3950	6.8 E5
1000	4510	6.1 E5

Table 5—12-lb/gal Bead, Compressive Young's Modulus

Confining Pressure (psi)	Effective Strength (psi)	Young's Modulus (psi)
0	5150	9.5 E5
500	6000	8.1 E5
1000	6150	1 E6

Table 6—Latex, Compressive Young's Modulus

Confining Pressure (psi)	Effective Strength (psi)	Young's Modulus (psi)
0	3500	5.6 E5
250	5250	8.9 E5
500	6000	9.4 E5

Poisson's Ratio Testing

Initial results of Poisson's ratio testing on these lightweight cement compositions were unexpectedly low. Continued Poisson's ratio testing during this test period to determine reasons for these low values confirmed the accuracy of these early results. The low Poisson's ratio values for these compositions are theorized to be related to the porosity of the specimens. Several published technical reports have documented this tendency for Poisson's ratio to be effectively lowered as porosity increases.

Another potential variable in Poisson's ratio testing is load rate. An investigation into the



effect of load rate on Poisson's ratio indicated that load rate does affect Poisson's ratio measurement (Table 7). Table 8 presents data generated with a load rate of 250 psi/min. While these values are lower than what has traditionally been considered acceptable, the data are generally positive.

CT scans performed on Poisson's ratio test specimens indicated a link between large voids or pore spaces and variable Poisson's ratio. This procedure will be included in future testing and samples with large voids will be discarded. CT scans are included in Appendix B.

Table 7—Effect of Load Rate on Poisson's Ratio

Load Rate	Poisson's Ratio
100 psi/min	0.1
250 psi/min	0.08
500 psi/min	-0.01

**Table 8—Poisson's Ratio
(50-psi confining pressure, 250 psi/min load rate)**

Slurry	Failure (psi)	ν Radial (ft ³ /sk)
Foam slurry (12-lb/gal)	3100	0.00
Bead slurry	4100	-0.01
Neat Class H slurry	6450	0.0012
SMS slurry	920	0.005
Type I slurry	6500	0.1

Strain Tests

The following data indicate that foam cement underwent the most anelastic strain during cycling. These results will be expanded upon in future anelastic strain testing.

Table 9—Strain Amounts/Cycling

Slurry	1000 psi	2000 psi	3000 psi	4700 psi
Foam slurry (12-lb/gal)	0.00261	0.00167	—	—
Bead slurry	0.00191	0.00158	0.00115	—
Class H slurry	0.00161	0.0015	0.00102	—
Type I slurry	0.00108	0.0008	0.00069	—

Rock Properties Testing

Results obtained with the Chandler Engineering device are generally in line with expected values. However, Poisson's ratio values are very high compared to results from this study and Young's modulus data are somewhat elevated compared to values measured with traditional methods.



Table 10—Data Obtained with Chandler Device

Slurry	Poisson's Ratio	Compressive Young's Modulus
Type I slurry	0.20	2.3 E6
Bead slurry	0.31	1.5 E6
Latex slurry	0.39	1.4 E6
Latex slurry with fibers	0.19	2.5 E6
Class H	0.24	2.2 E6
Class H slurry with fibers	0.25	2.3 E6

Table 11—Data Obtained with

Slurry	Poisson's Ratio	Compressive Young's Modulus
Type I slurry	0.1	1.7 E6
Bead slurry	0.0	9.5 E5
Latex slurry	—	5.6 E5
Latex slurry with fibers	—	—
Class H slurry	0.0	1.0 E6
Class H slurry with fibers	—	—

The data in Table 12 were gathered to illustrate the variations between radial measurement techniques. Note that wide variations exist between Poisson's ratios measured with point measurement devices, even among measurements taken from the same sample.



Table 12—Effects of Variable Confinement and Load Rates on Rock Properties

Slurry	Length (in.)	Diameter(in.)	Saturated Wt (g)	Test Type	Confining Stress	Failure (psi)	Young's Modulus x(E6)	ν Circumferential	ν Radial Point Meas. 1	ν Radial Point Meas. 2	Test Rate (psi/min)
Foam	2.98	1.4	126.39	confine fail	50 psi	3,100	0.432	-5.00E-05	1.6	1.7	250
Bead	3.03	1.4	113.75	confine fail	50 psi	4,100	0.616	-0.01	-4.6	0.26	250
Class H	2.89	1.4	156.82	confine fail	50 psi	6,450	1	0.0012	3.75	-0.79	250
SMS	3.01	1.4	111.08	confine fail	50 psi	921	0.086	0.005	1.92	-0.95	250
Type I	3.08	1.4	152.1	confine fail	50psi	6,500	1	0.1	-1.8	-0.05	250



Shear Bond Tests

Results of shear bond testing (Table 13) indicated that the bond was degraded extensively both by pressure cycling and temperature cycling. This degradation seemed to be aggravated by the soft formation. Modifications are being made to the shear bond test method so that the results of future tests will be more comparable with the results from annular seal tests.

Table 13—Shear Bond Strengths (psi)

System	Simulated Formation	Type I Slurry	Foam Slurry	Bead Slurry	Latex Slurry
Baseline	hard	1194	127/98	109/78	—
	soft	198	233	143	223
Temperature-Cycled	hard	165	299/215	191/269	—
	soft	72	7	56	149
Pressure-Cycled	hard	194/106	276/228	294/170	—
	soft	23	22*	23*	11

* Visual inspection revealed samples were cracked.

Annular Seal Tests

Results presented in Table 14 indicate that in cyclic testing, all specimens tested in a soft formation simulation failed whereas all specimens tested in a hard-formation simulation maintained a seal. A simulated formation with intermediate strength is needed to further differentiate seal effectiveness. To determine the failure point in the simulated hard-formation tests, additional stresses must be imposed by heating or pressure application.

Table 14—Annular Seal Tests

Condition Tested	Formation Simulated	Type I Slurry	Foamed Slurry	Bead Slurry
Initial Flow	Hard	0 Flow	0 Flow	0 Flow
	Soft	0 Flow	0.5 (md)	0 Flow
Temperature-Cycled	Hard	0 Flow	0 Flow	0 Flow
	Soft	0 Flow	123 md	43 md*
Pressure-Cycled	Hard	0 Flow	0 Flow	0 Flow
	Soft	27 md	0.19 md*	3 md

* Visual inspection revealed samples were cracked.



Appendix A—Test Procedures

Following the procedures set forth in API Spec. 10¹, thickening-time tests were performed on all cement systems. The test conditions started at 80°F and 600 psi, and were ramped to 65°F and 5,300 psi within 48 minutes.

Modified Blending Procedures

Some preparation and testing methods were modified to adapt to the lightweight bead and foamed slurries.

The following blending procedure was used for the bead slurry. It was modified to minimize bead breakage due to the high shear of API blending procedures.

1. Weigh out the appropriate amounts of the cement, water, and beads into separate containers.
2. Mix the cement slurry (without beads) according to Section 5.3.5 of API Spec. 10¹.
3. Pour the slurry into a metal mixing bowl and slowly add beads while continuously mixing by hand with a spatula. Mix thoroughly.
4. Pour the slurry back into the Waring blender and mix at 4,000 rev/min for 35 seconds to evenly distribute the contents.

Testing methods for the foamed slurries were also modified. For example, thickening time is performed on unfoamed slurries only. Because the air in the foam does not affect the hydration rate, the slurry is prepared as usual per API Spec. 10¹ and then the foaming surfactants are mixed into the slurry by hand without foaming the slurry.

Free-Fluid Testing

The free-fluid testing that was performed on the Type I cement, foamed cement and bead slurries came from API Spec. 10¹ (Table A1). The free-fluid procedure, also referred to as operating free water, is used with a graduated cylinder that is oriented vertically.

Table A1—Free Fluid Test Results

Slurry System	Thickening Time to 100 Bc (hr:min)	Percentage of Free Fluid
Neat	4:38	0.8
Foamed	3:42	0.0
Bead	5:04	0.8



Compressive Strength Testing

The compressive strengths were derived using the 2-in. cube crush method specified in API Spec. 10¹. The samples were cured in an atmospheric water bath at 45°F. The reported values were taken from the average of three samples.

Sample Curing

Test specimens for rock properties testing are mixed in a Waring blender and poured into cylinder molds. The samples are then cured for seven days in an atmospheric water bath set at 45°F.

Performance test-fixture molds are filled with cement mixed in the same manner. These fixtures are also cured in a 45°F water bath for seven days prior to testing.

Young's Modulus and Poisson's Ratio Testing

Traditional Young's modulus testing is to be performed using ASTM C469², Standard Test Method for Static Modulus of Elasticity (Young's Modulus) and Poisson's Ratio of Concrete in Compression with a modified load rate.

The following procedure is used:

1. Inspect each sample for cracks and defects. Evaluate a CT scan of each sample for excessively large pores. Discard any defective samples.
2. Cut each sample to a length of 3.0 in.
3. Ground the sample's end surfaces to create a flat, polished surface with perpendicular ends.
4. Measure the sample's physical dimensions (length, diameter, weight).
5. Place the sample in a Viton jacket.
6. Mount the sample in the Young's modulus testing apparatus.
7. Verify that the pore lines on the end caps of the piston are open to atmosphere to prevent pore-pressure buildup.
8. Bring the sample to 100-psi confining pressure and axial pressure, and allow the sample to stand for 15 to 30 minutes until stress and strain are at equilibrium. (In case of an unconfined test, apply only axial load.)
9. Increase the axial and confining stress at a rate of 25 to 50 psi/min to bring the sample to the desired confining stress condition, and allow the sample to stand until stress and strain reach equilibrium.
10. Subject the sample to a constant stress rate of 250 psi/min.
11. Measure the radial strain with a circumferential band instrumented with a strain gauge rather than multiple point deflections.
12. After the sample fails, bring the system back to the atmospheric stress condition.
13. Remove the sample from the cell and store it.



Specimens from each composition under investigation will first be tested in an unconfined (50-psi radial stress) condition to determine unrestrained yield and mechanical properties. A minimum of three samples will be tested for each test condition.

Anelastic Strain and Cycling

Anelastic strain testing is a variation of hydrostatic testing and is designed to allow a more accurate evaluation of permanent strain resulting from stressing different test compositions. This procedure standardizes confining stress at 500 psi and calls for samples to be cycled to 25%, 50%, and 75% of each composition's compressive strength under that confining stress. Measurement of anelastic strain with cycling provides a more comparable value of each composition's performance.

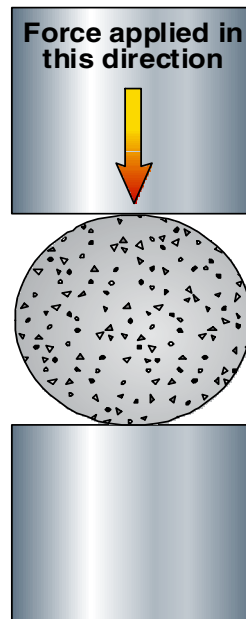
The exact procedure involves compression-testing a sample to failure in the load cell with 500-psi confining stress. Once this value is determined (from a Young's modulus test), additional samples will be tested by applying an axial load equal to 25%, 50%, and 75% of the failure load and cycling until the samples fail. A cyclic loading rate will be maintained at 250 psi/min and confining force will be maintained at 500 psi. Plastic deformation will be measured at the end of each cycle. Results will include cycles to failure and anelastic strain per cycle. CT scans will be performed on each sample prior to testing to rule out the possibility of large voids in the sample.

Tensile Strength and Tensile Young's Modulus

Tensile strength is to be tested using ASTM C496³ (Standard Test Method for Splitting Tensile Strength of Cylindrical Concrete Specimens). For this testing, the specimen dimensions were 1.5 in. in diameter by 1 in. long. **Figure A1** shows a general schematic of how a specimen is oriented on its side when tested. Force is applied by constant displacement of the bottom plate at a rate of 1 mm every 10 minutes. Change in the specimen diameter can be calculated from the test plate displacement. The (tensile) strength of the specimen during the test can be graphed along with the diametric strain (change in diameter/original diameter) to generate the tensile Young's modulus. A minimum of three samples per composition will be tested. CT scans of samples will be examined for defects prior to testing.



Figure A1—Sample Orientation for ASTM C496-90 Testing



Annular Seal Testing Procedure

Cements are mixed and poured into specified molds and cured for 7 days in an 80°F water bath. After curing, three specimens from each test composition and condition are tested.

Three separate molds simulating soft, intermediate, and hard formations are used to prepare samples:

- The soft formation mold is a soft gel mold that surrounds the cement slurry and provides a semi-restricting force on the outside of the core while it cures.
- The intermediate specimen is designed with a 3-in. diameter Schedule 40 PVC pipe as the outer containment.
- The hard formation mold features a 3-in. diameter Schedule 40 steel pipe as the outer containment, giving the cement slurry a restricting force outside of the core.

The following annular seal test procedures are all designed for use with the annular seal apparatus. The samples produced from the three mold types are each tested with a different procedure. In all annular seal testing, stress was applied to the specimens by applying hydraulic pressure to the inner pipe or heating the inner pipe.

Simulated Soft-Formation Test

1. After the core is cured, place the core inside the gel mold sleeve.
2. Place the core and sleeve inside the Pipe-in-Soft steel cell.
3. With the core inside the cell, make sure that both ends of the core are supported with O-rings.



4. Attach the end plates to tighten the O-rings and close off leaks that might be present.
5. Using water, pressurize the exterior circumference of the sleeve to 25 psi. Once the pressurized water is applied to the cell, check for leaks on the ends of the cell.
6. Using the cell's end caps, cap off both ends of the steel cell. One end cap has a fitting that allows for N₂ gas to be applied to the cell; the other end cap allows for the gas to exit the cell.
7. Attach the pressure inlet line to the bottom of the steel cell, and attach the pressure outlet line to the top of the cell.
8. Apply pressure to the inlet line. (Do not exceed 20 psig.)
9. Measure the flow out of the outlet line with flowmeters.

Simulated Hard-Formation Test

1. After the core is cured inside the steel pipe, cap off each end of the pipe with a steel end cap. Each end cap has a fitting that allows for gas to enter or exit the pipe.
2. Attach the pressure inlet line to the bottom of the steel cell, and attach the pressure outlet line to the top of the cell.
3. Apply pressure to the inlet line. (Do not exceed 20 psig.)
4. Measure the pressure out of the outlet line with flowmeters.

Simulated Moderate-Strength Formation Test

The hard formation test procedure can be used for this test by replacing the outer pipe with Schedule 40 PVC.

Temperature and Pressure Cycling

Thermal cycling was simulated by inserting heaters into the inner pipe and heating the inner pipe from 80°F to 180°F, then allowing the pipe to cool to 80°F. Three specimens were tested for each composition. The temperature schedule in Table A2 was used in the testing.

**Table A2—Temperature Schedule
for Thermal Cycling**

Hours	Temperature (°F)
1	94
2	108
3	121
4	135
5	149
6	163
7	176
8	190



For thermal testing, a thicker-walled inner pipe must be used to provide more steel volume for expansion. This change is necessary to accommodate increased stress application to induce failure in all samples. The new inside pipe will be 1.5-in. Schedule 80 pipe and the outer containment diameter will be increased to 5 in.

For pressure cycling, hydraulic pressure was applied to the inner pipe. For the initial cycle, pressure was increased from 0 to 500 psi. Pressure was then released to 0 and flow measurements were made. Additional cycles were run by increasing the upper pressure limit by 500 psi (0 to 1,000 psi, 0 to 1,500 psi, 0 to 2,000 psi, etc.) up to a maximum of 10,000 psi, and flow measurements were made at the end (0) point of each cycle. If the sample did not fail at or below 10,000 psi of pressure, the sample was cycled at 10,000 psi a minimum of 5 times. Three specimens will be tested for each composition.

Shear Bond Strength Testing

Shear bond strength tests are used for investigating the effect of restraining force on shear bond. Samples are cured in a hard formation configuration (**Figure A2**) and in a soft formation configuration (**Figure A3**). The hard configuration consists of a sandblasted internal pipe with an outer diameter (OD) of 1 1/16 in. and a sandblasted external pipe with an internal diameter (ID) of 3 in. and lengths of 6 in. A contoured base and top are used to center the internal pipe within the external pipe. The base extends into the annulus 1 in. and cement fills the annulus to a length of 4 in. The top 1 in. of annulus contains water.

Figure A2—Cross-Section of Pipe-in-Pipe Configuration for Shear Bond Tests

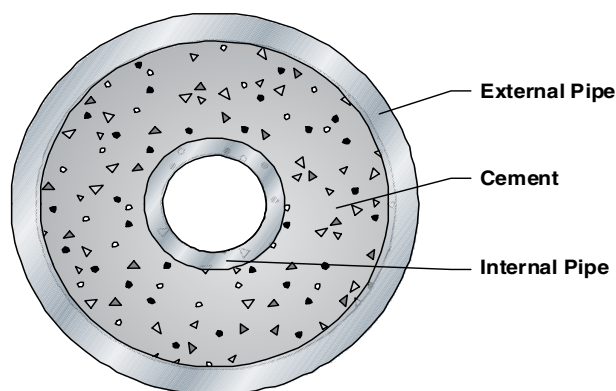
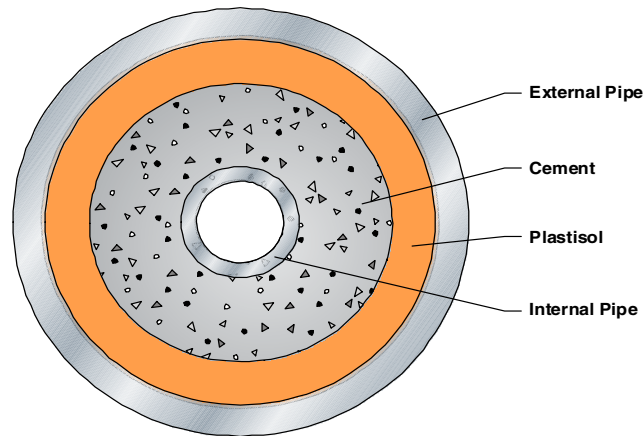




Figure A3— Cross-Section of Pipe-in-Soft Configuration for Shear Bond Tests



In the soft formation shear bond tests, Plastisol allows the cement to cure in a less-rigid, lower-restraint environment. Plastisol is a mixture of a resin and a plasticizer that creates a soft, flexible substance. This particular Plastisol blend (PolyOne's Denflex PX-10510-A) creates a substance with a hardness of 40 duro.

The soft formation configuration contains a sandblasted external pipe with a 4-in. ID. A molded Plastisol sleeve with a 3-in. ID and uniform thickness of 0.5 in. fits inside this external pipe. A sandblasted internal pipe with an OD of 1 1/16 in. is then centered within the Plastisol sleeve. The pipes and sleeve are 6 in. long. The base of the exterior pipe extends into the annulus 1 in. and cement fills the annulus to a height of 4 in. between the Plastisol sleeve and the inner 1 1/16 -in. pipe. The top inch of annulus is filled with water.

The intermediate formation test specimen will be configured just as the hard formation except the outer pipe is made of PVC.

Cycling tests for the shear bond specimens were performed according to the following test schedules:

Pressure Cycling Schedule

1. Cure specimens for 14 days at 45°F.
2. Apply 5000 psi hydraulic pressure to the inner pipe and maintain for 10 minutes.
3. Release the pressure and wait 10 minutes.
4. Repeat the cycle four more times.
5. Perform the shear bond test.

Temperature Cycling Schedule

1. Cure specimens for 14 days in a 45°F water bath.

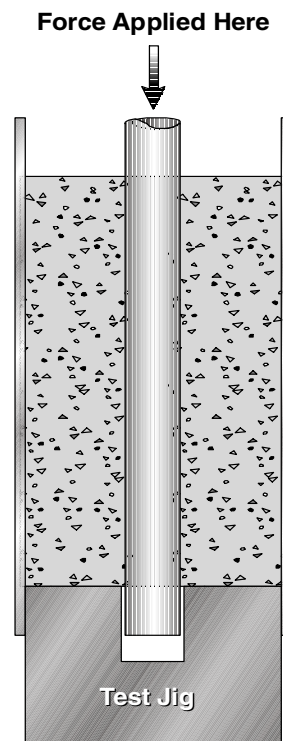


2. Move specimens from a 45°F water bath to a 96°F water bath for 1 hour.
3. Place specimens in a 180°F water bath for 4 hours.
4. Place specimens in a 96°F water bath for 1 hour.
5. Return specimens to a 45°F bath.
6. Repeat the cycle four more times.
7. Perform the shear bond test.

A new test procedure for future shear bond testing will allow the comparison of results with annular seal test results. After failure is noted in the annular seal test, the exact pressure or temperature cycle sequence will be repeated for the shear bond specimens. Shear bond will be measured after the cycling to determine the level of bond remaining.

The shear bond measures the stress necessary to break the bond between the cement and the internal pipe. This was measured with the aid of a test jig that provides a platform for the base of the cement to rest against as force is applied to the internal pipe to press it through (**Figure A4**). The shear bond force is the force required to move the internal pipe. The pipe is pressed only to the point that the bond is broken; the pipe is not pushed out of the cement. The shear bond strength is the force required to break the bond (move the pipe) divided by the surface area between the internal pipe and the cement.

Figure A4—Configuration for Testing Shear Bond Strength



Cement Column Seal Tests

Eight-foot lengths of 2-in. Schedule 40 pipe are mounted vertically and fitted with caps at



the top and bottom equipped with pressure input and outlet ports. The bottom of each pipe is filled with 6 in. of 20- to 40-mesh sand to provide an open base for gas injection. Two fixtures are filled with one of four different cement slurries (bead, Type 1, latex, and SMS). Samples are capped with water and cured for seven days under 1000 psi of pressure. After the samples are cured, 100 psi of pressure is applied to the bottom of each fixture and any flow through the column is monitored.



Appendix B—Test Data

Graphical data for all mechanical properties tests performed in this investigation are presented in this appendix.



Table B1—Hydrostatic Cycle Test

Slurry	Length (in.)	Diameter (in.)	Saturated Wt (g)	Young's Modulus x(E6)	Axial Strain at 1000 psi (ramp up)	Axial Strain at 1000 psi (ramp down)	Net Axial Strain at 1000 psi	Axial Strain at 2000 psi (ramp up)	Axial Strain at 2000 psi (ramp down)	Net Axial Strain at 2000 psi	Test Rate (psi/min)
Foam-2	3	1.4	125.2	0.65	0.00375	0.00636	0.00261	0.00542	0.00709	0.00167	250
Bead-1	3.1	1.4	114	2	0.0079	0.00981	0.00191	0.00846	0.01004	0.00158	250
Class H-1	3.1	1.4	159.1	2	0.00139	0.003	0.00161	0.00189	0.00339	0.0015	250
Neat A-1	3.1	1.4	153.9	3	0.00116	0.00224	0.00108	0.00147	0.00227	0.0008	100

Slurry	Length (in.)	Diameter (in.)	Saturated Wt (g)	Young's Modulus x(E6)	Axial Strain at 3000 psi (ramp up)	Axial Strain at 3000 psi (ramp down)	Net Axial Strain at 3000 psi	Axial Strain at 4700 psi (ramp up)	Axial Strain at 4700 psi (ramp down)	Test Rate (psi/min)
Foam-2	2.99	1.4	125.2	0.65	0.00708	0.00708	—	—	—	250
Bead-1	3.06	1.4	114.02	2	0.00891	0.01006	0.00115	0.01002	0.01002	250
Class H-1	3.1	1.4	159.06	2	0.00233	0.00335	0.00102	0.00318	0.00318	250
Neat A-1	3.1	1.4	153.85	3	0.00159	0.00228	0.00069	0.00177	0.00177	100



Figure B1—Plot of tensile strength and Young’s modulus results for latex slurry with fibers (sample 1), Type 1 slurry with fibers (sample 2), and latex slurry (sample 3).

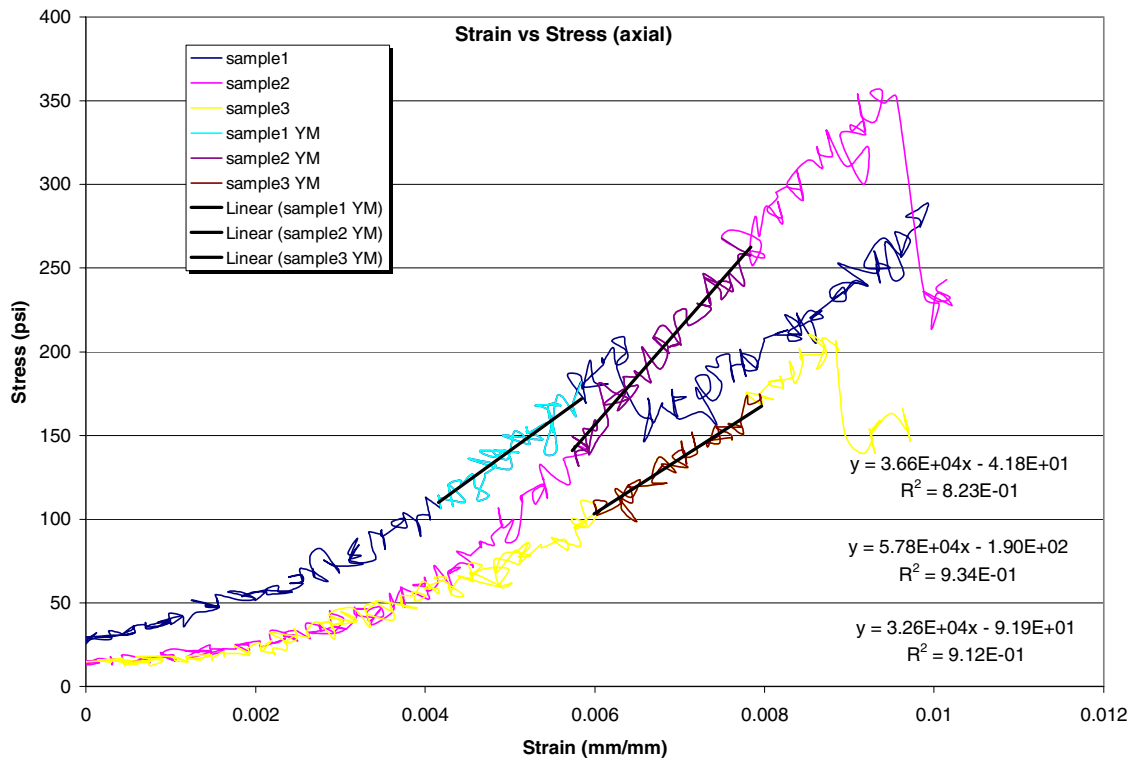




Figure B2—Plot of tensile strength and Young's modulus results for neat Type 1 slurry cured in a confined state.

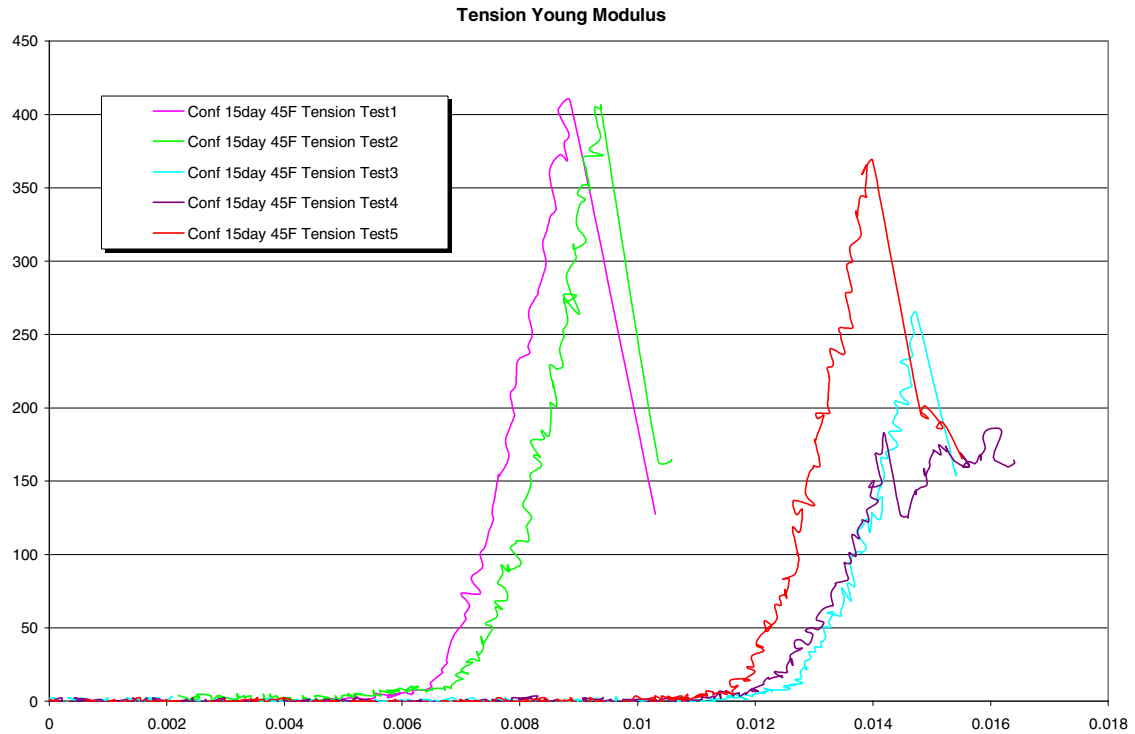




Figure B3—Plot of tensile strength and Young’s Modulus results for 12-lb/gal foam slurry.

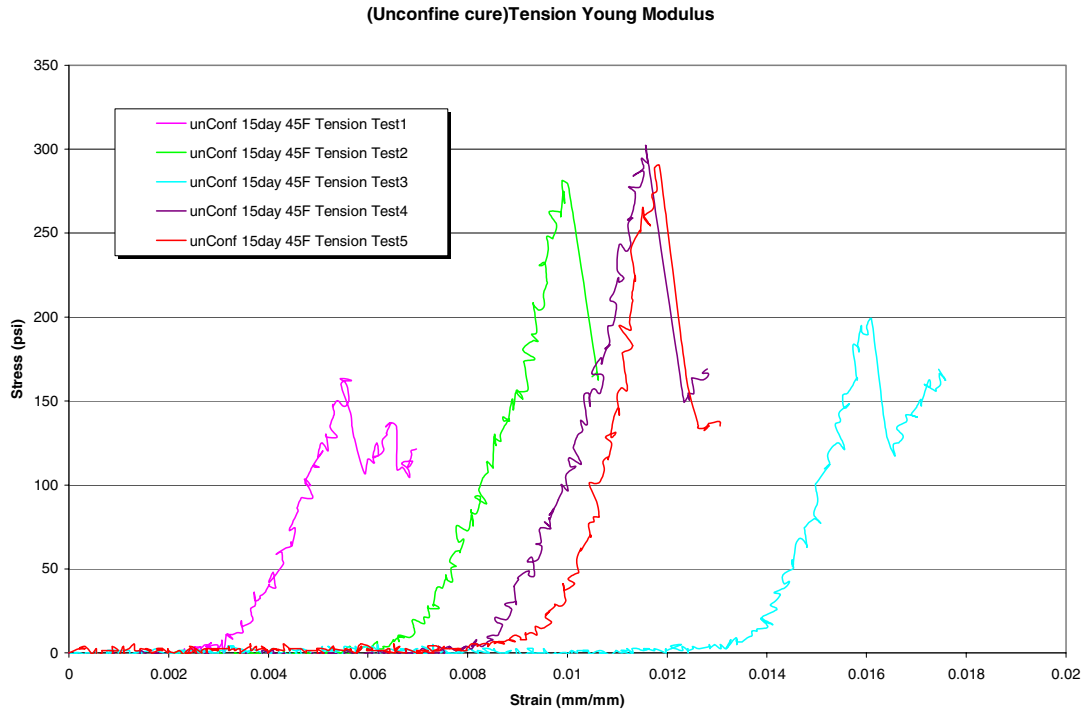


Figure B4—Plot of compressive Young’s modulus for Type 1 slurry at 0-psi confining pressure.

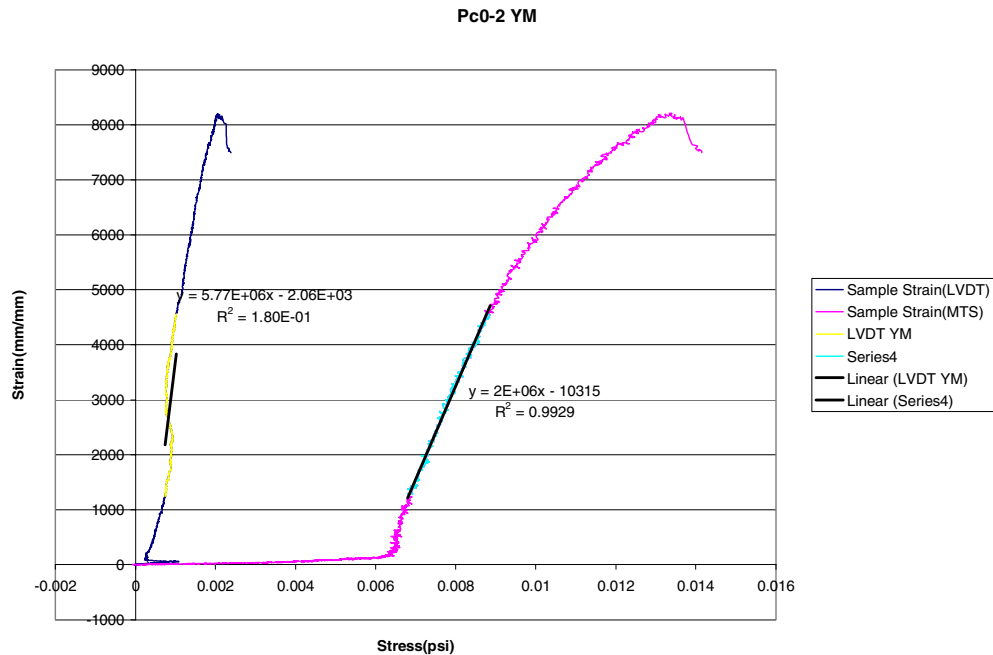




Figure B5—Plot of compressive Young's modulus for Type 1 slurry at 1500-psi confining pressure.

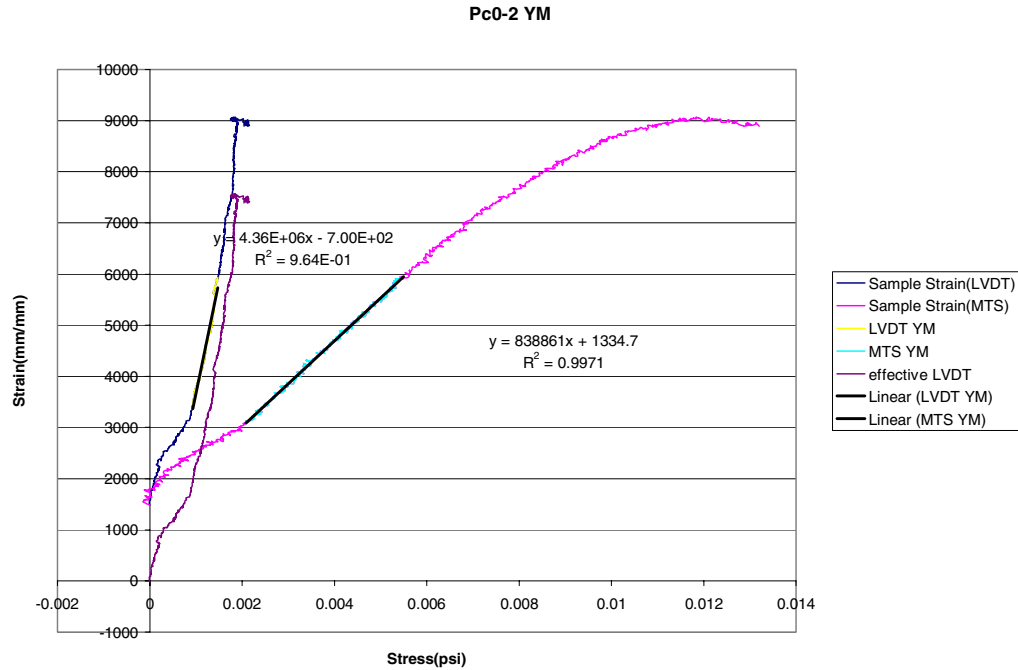


Figure B6— Plot of compressive Young's modulus for Type 1 slurry at 5000-psi confining pressure.

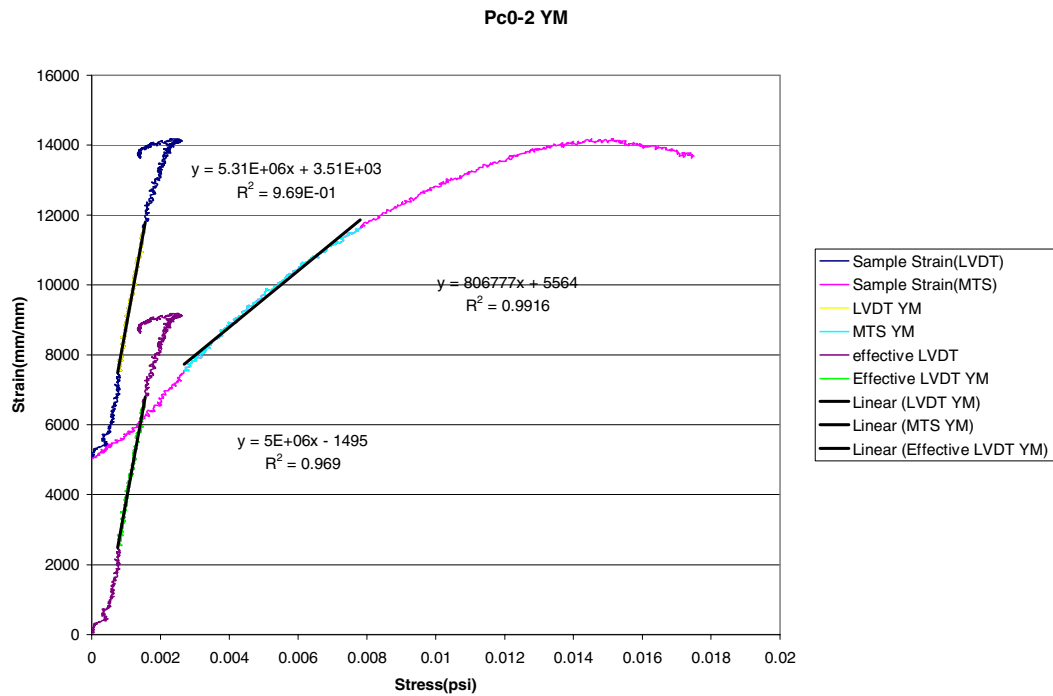




Figure B7— Plot of compressive Young's modulus for 12-lb/gal foam slurry at 0-psi confining pressure.

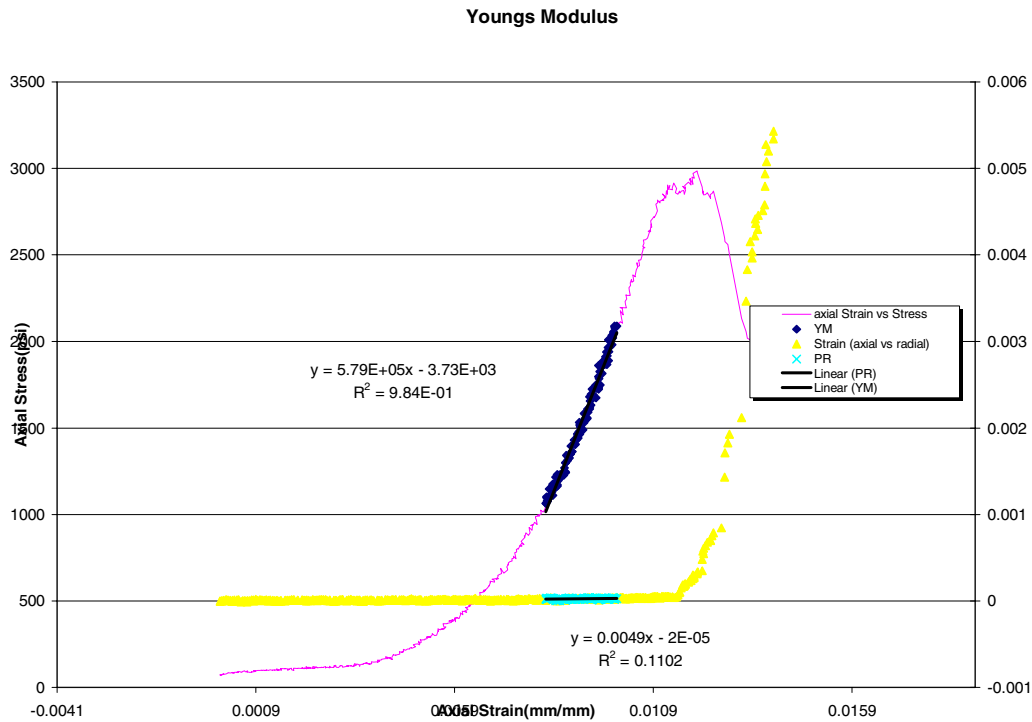


Figure B8— Plot of compressive Young's modulus for 12-lb/gal foam slurry at 500-psi confining pressure.

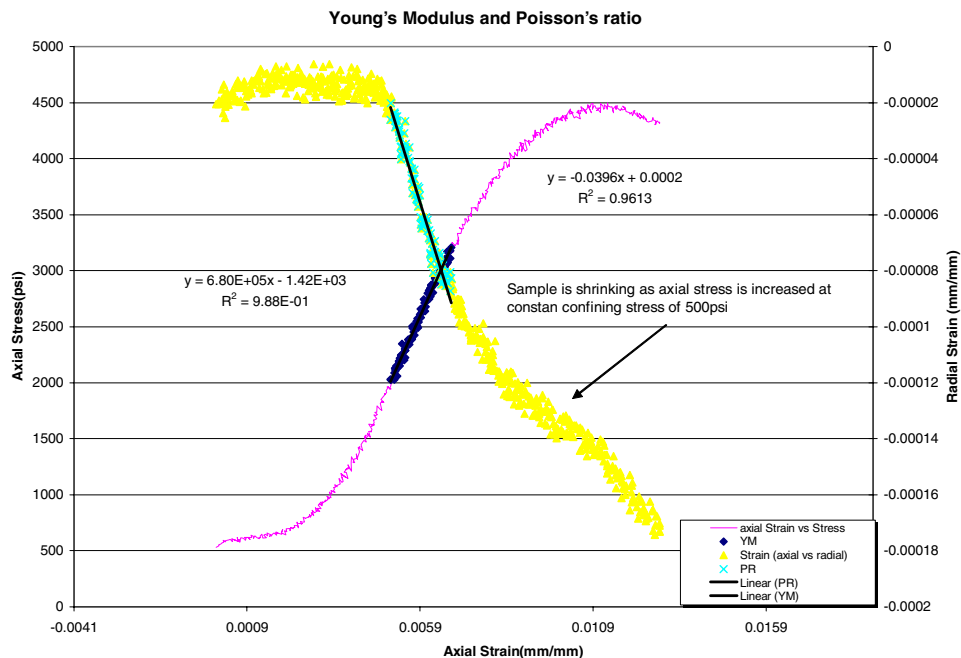




Figure B9— Plot of compressive Young's modulus for 12-lb/gal foam slurry at 1000-psi confining pressure.

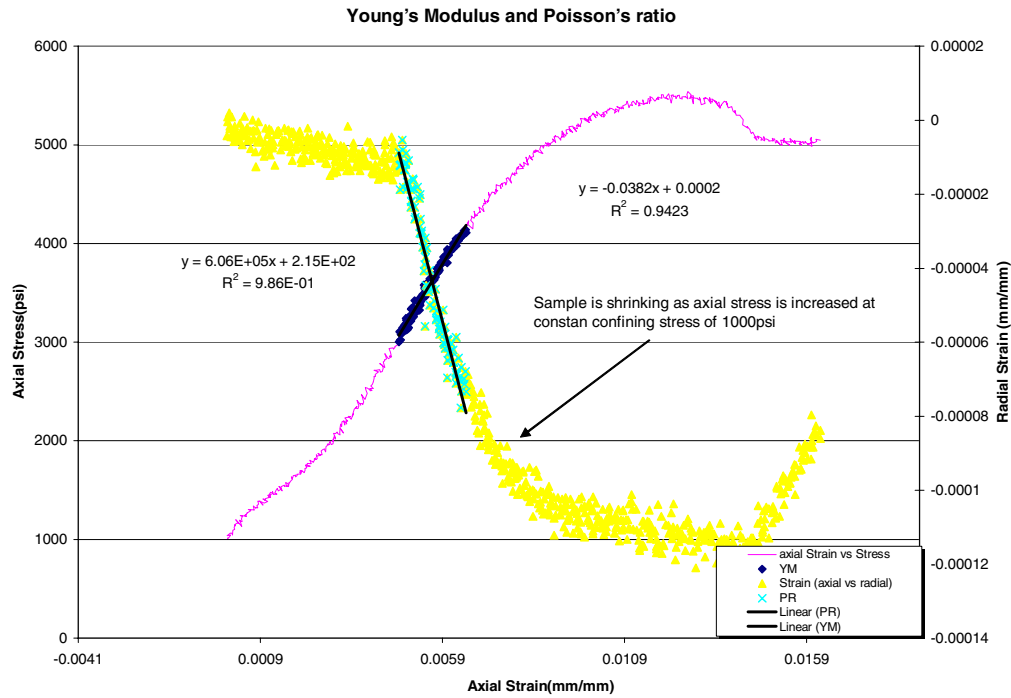


Figure B10— Plot of compressive Young's modulus for bead slurry at 0-psi confining pressure.

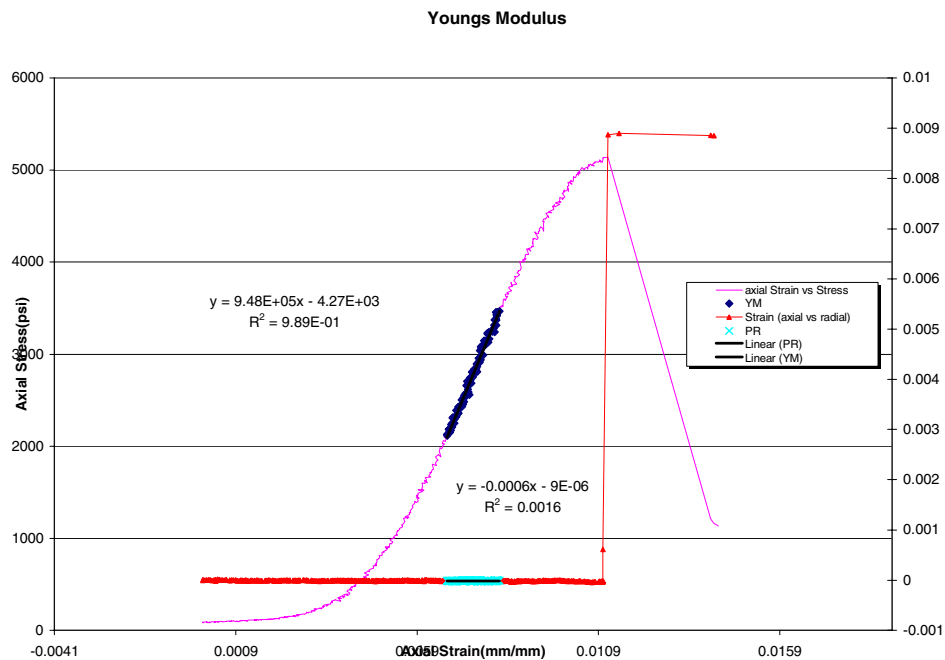




Figure B11— Plot of compressive Young's modulus for bead slurry at 500-psi confining pressure.

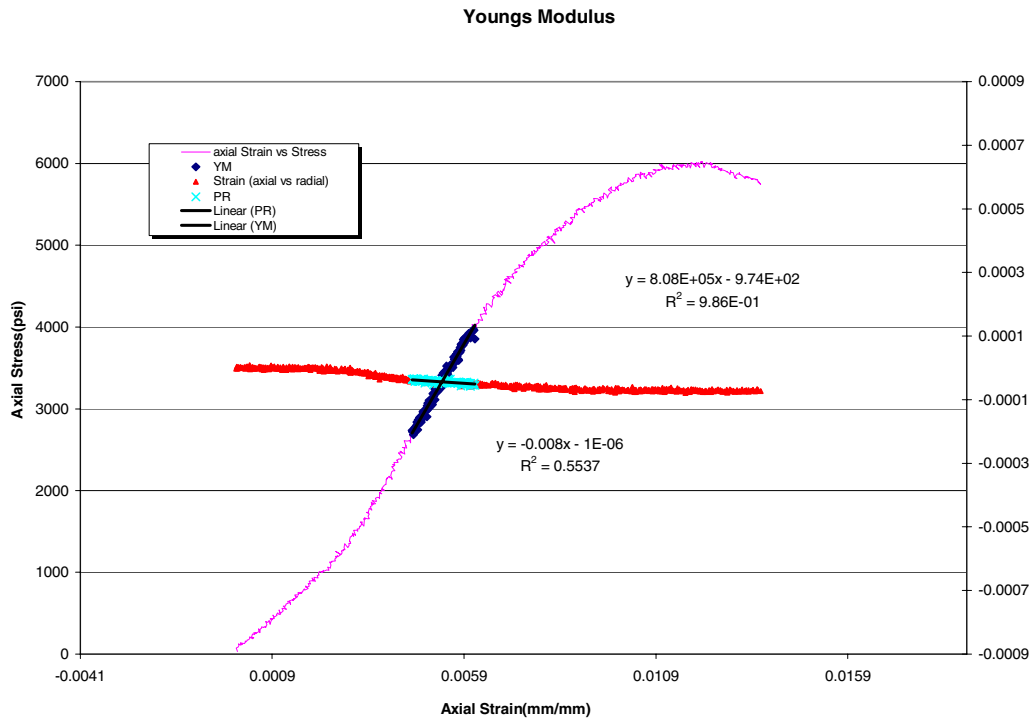


Figure B12— Plot of compressive Young's modulus for bead slurry at 1000-psi confining pressure.

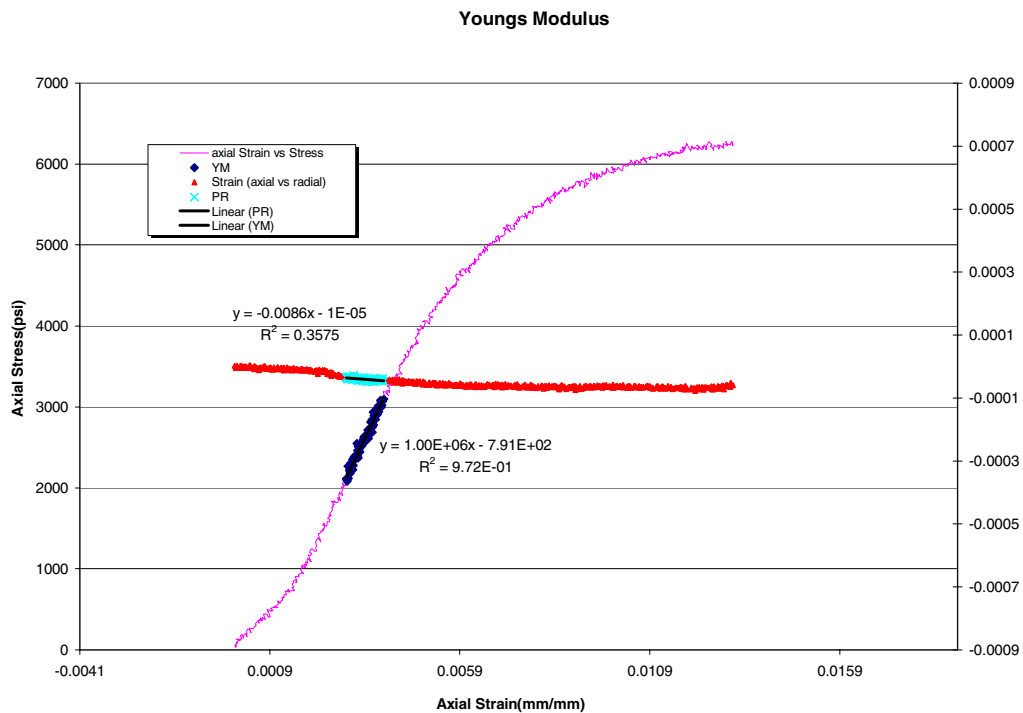




Figure B13— Plot of compressive Young's modulus for latex slurry at 0-psi confining pressure.

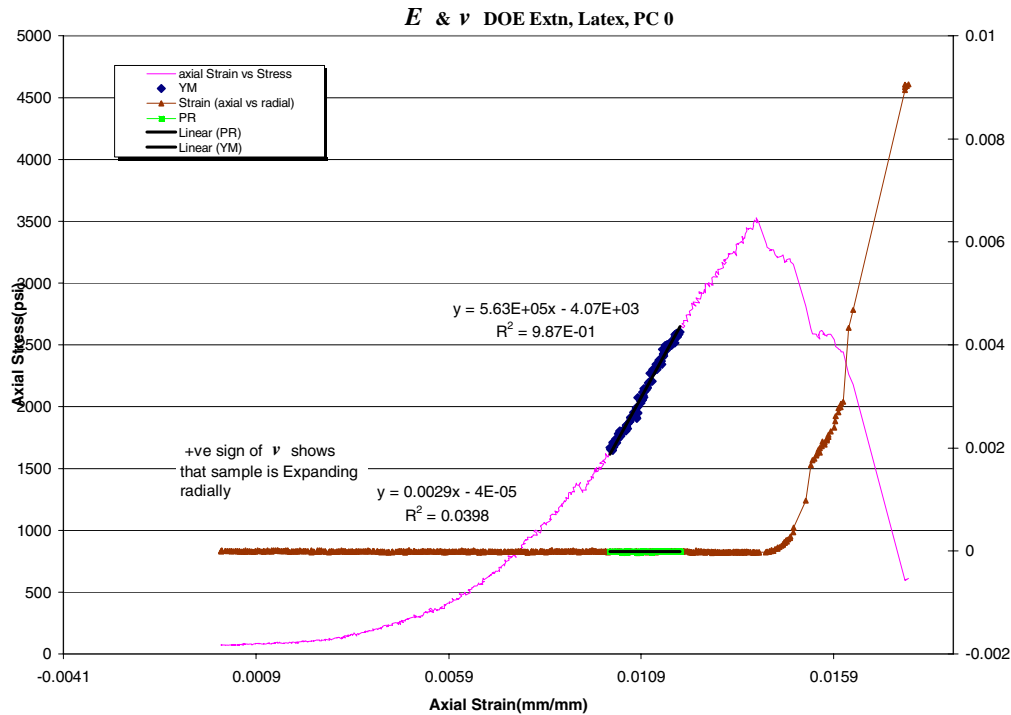


Figure B14— Plot of compressive Young's modulus for latex slurry at 250-psi confining pressure.

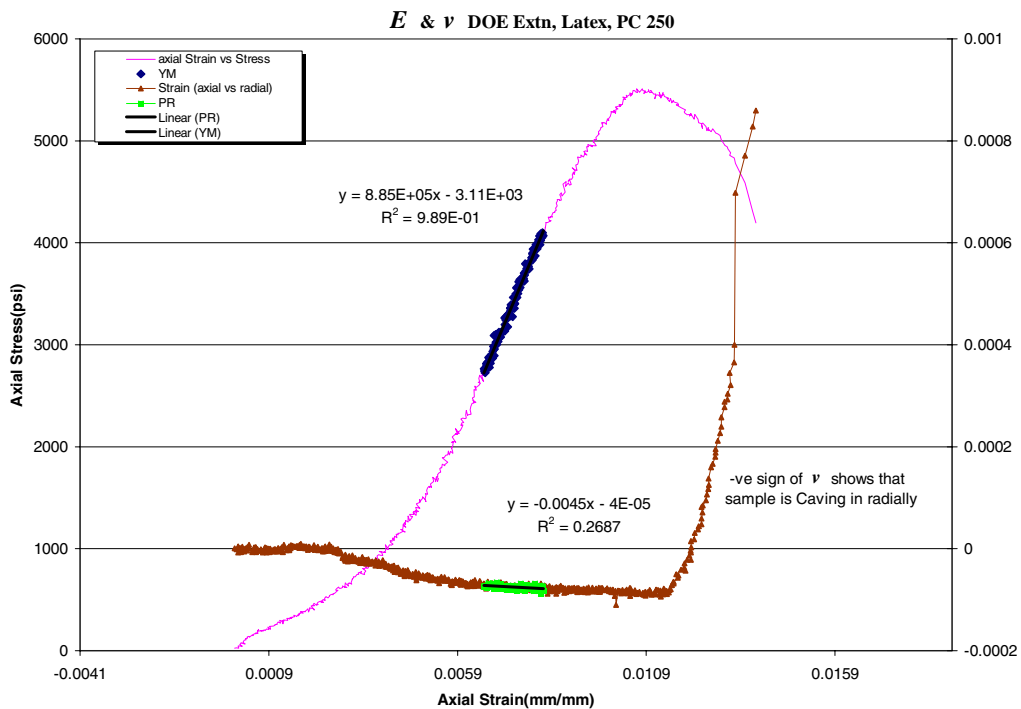




Figure B15— Plot of compressive Young’s modulus for latex slurry at 500-psi confining pressure.

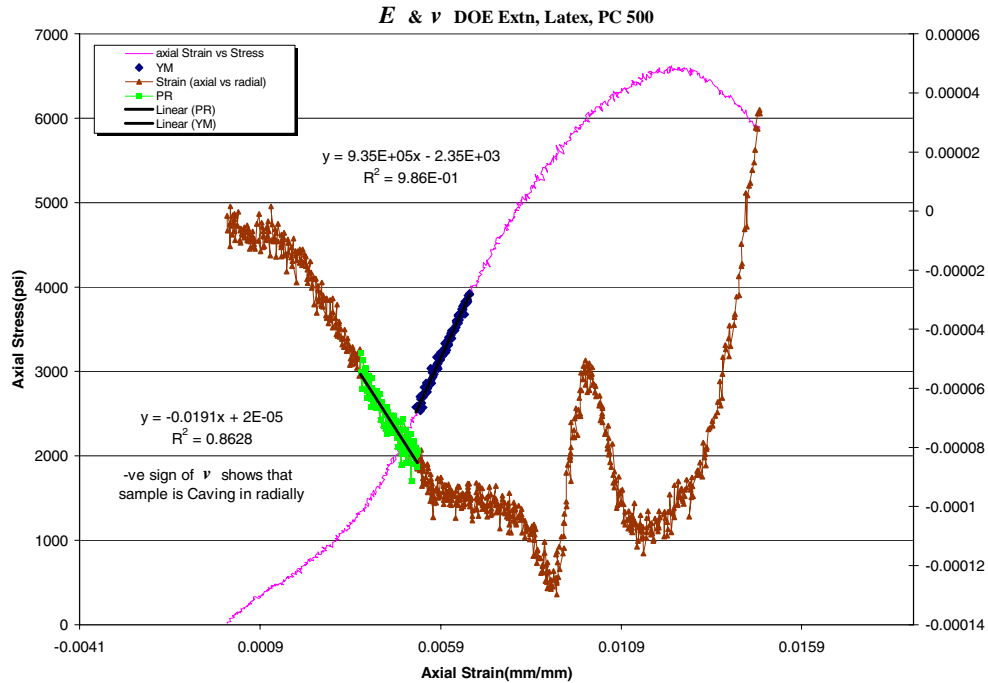


Figure B16—Young’s modulus measurements for Type I slurry at 500-psi confining stress and a 100-psi/min load rate.

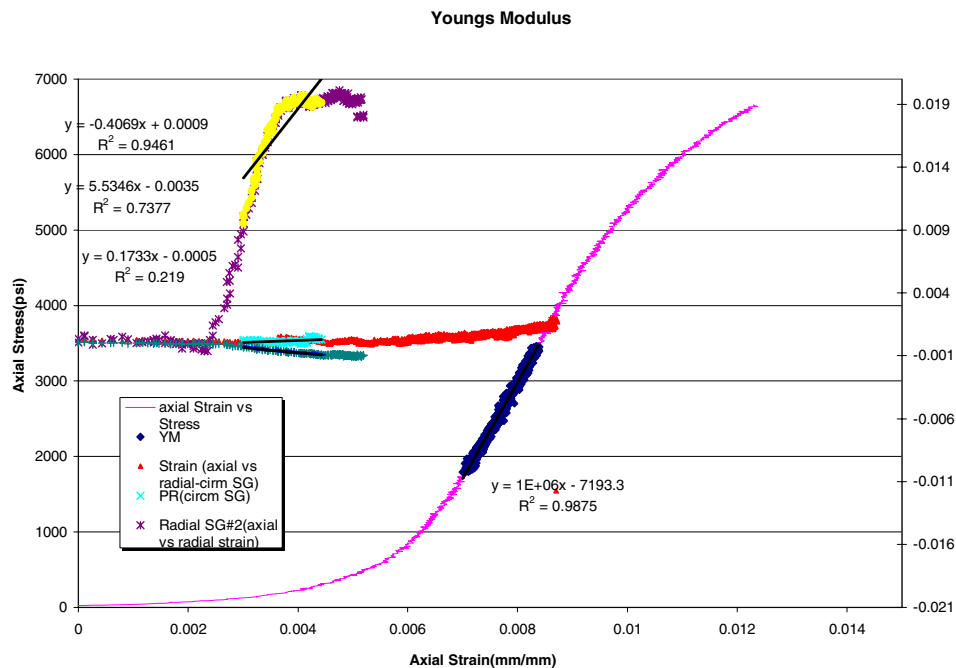




Figure B17—Young’s modulus measurements for Type I slurry at 500-psi confining stress and a 250-psi/min load rate.

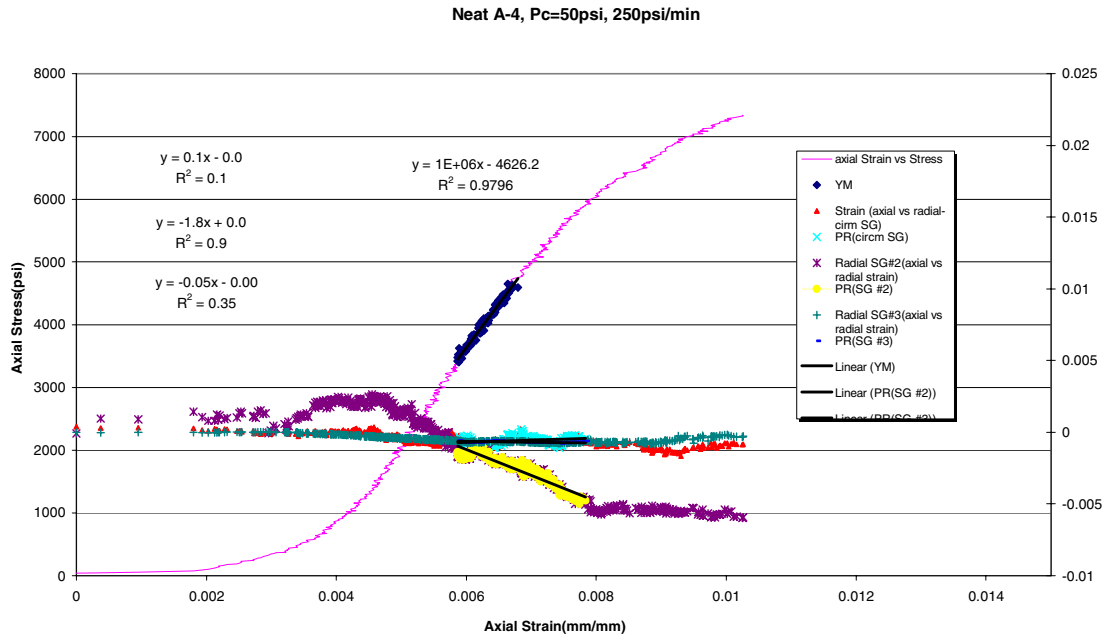


Figure B18—Young’s modulus measurements for Type I slurry at 500-psi confining stress and a 500-psi/min load rate.

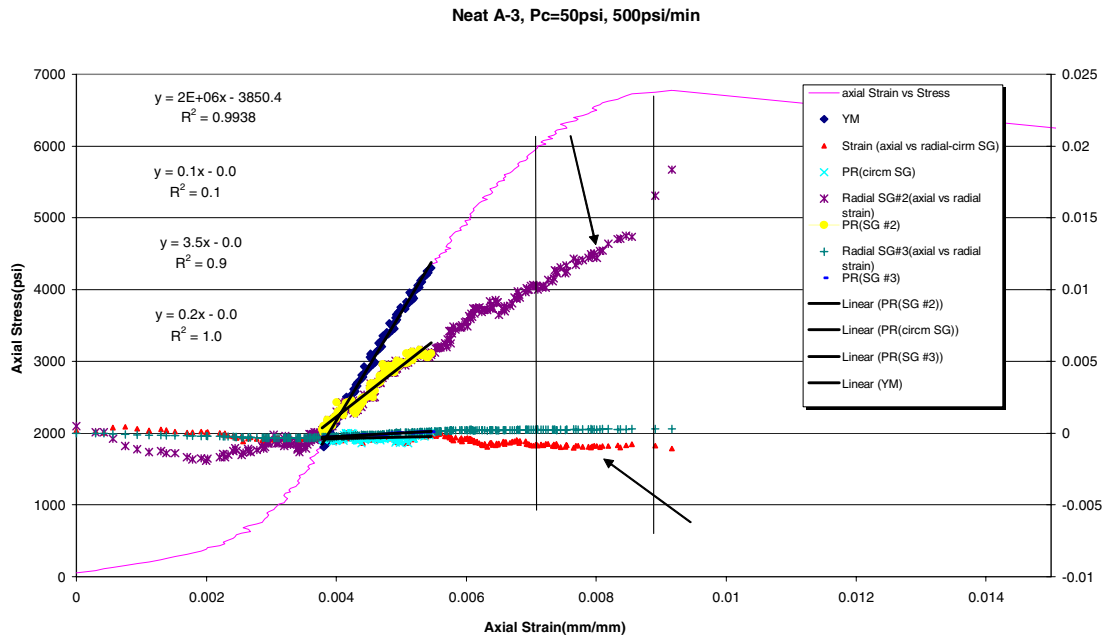




Figure B19—Hydrostatic cycling data for bead slurry showing anelastic strain.

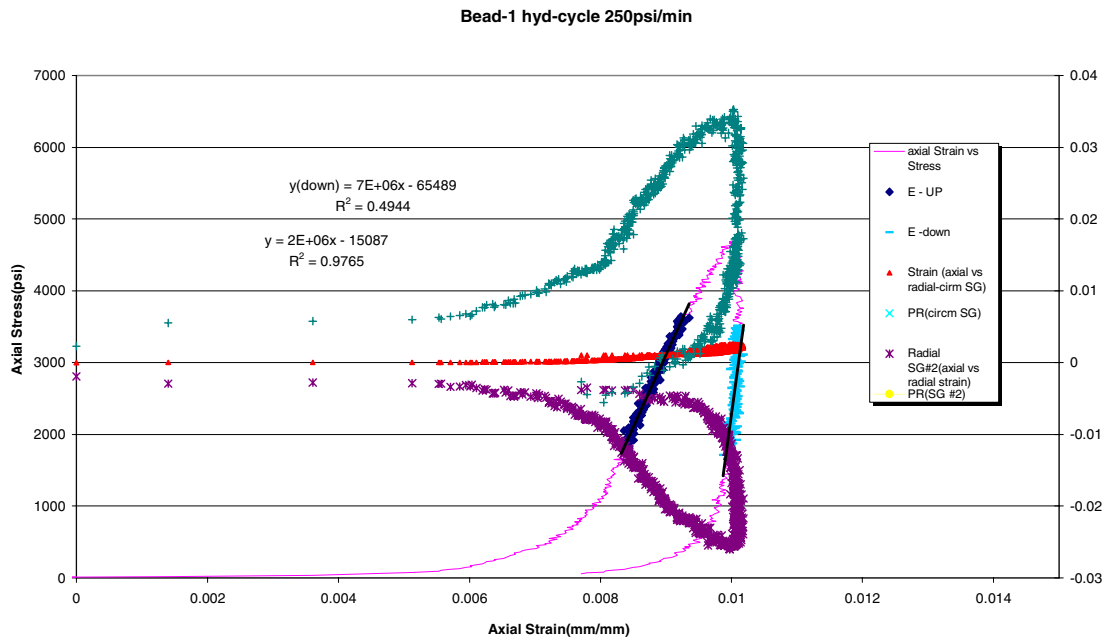


Figure B20— Hydrostatic cycling data for Class H slurry showing anelastic strain.

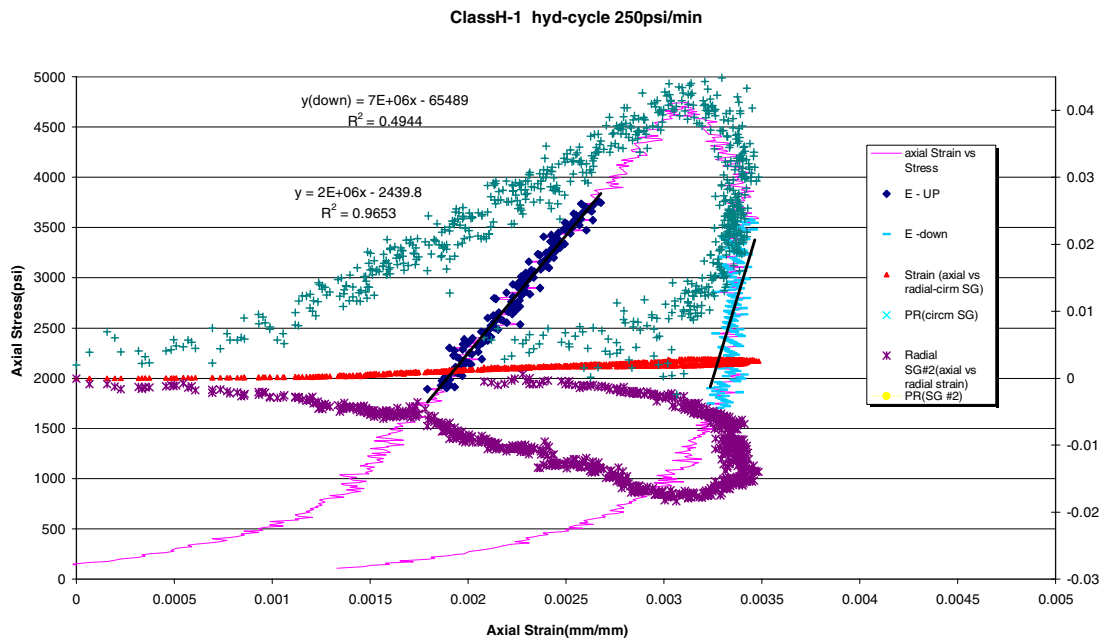




Figure B21— Hydrostatic cycling data for 12-lb/gal foam slurry showing anelastic strain.

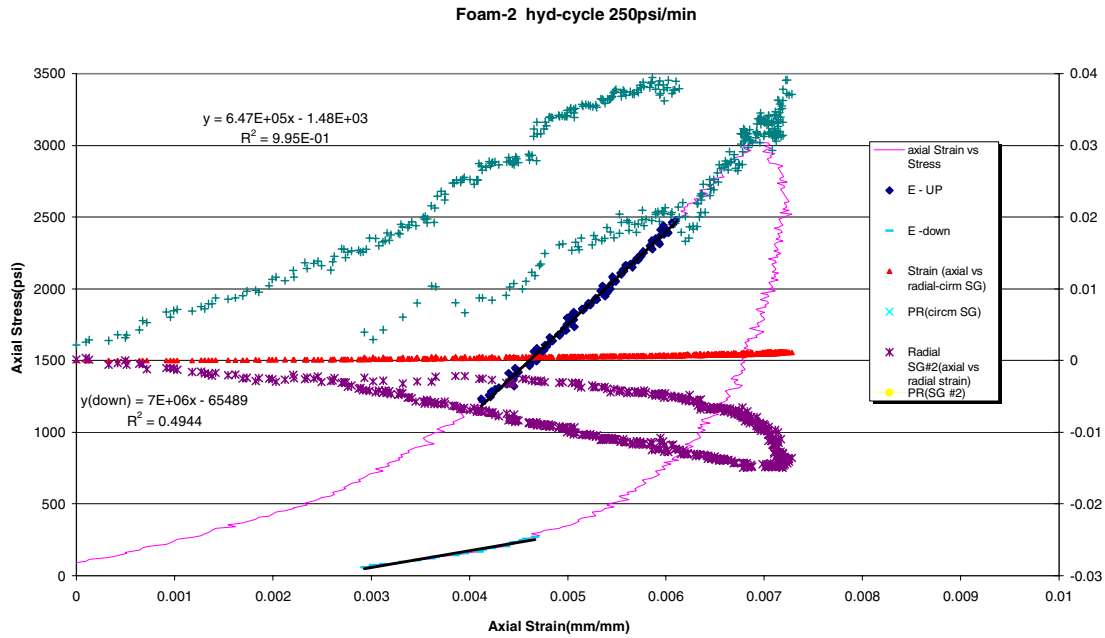


Figure B22— Hydrostatic cycling data for Type I slurry showing anelastic strain.

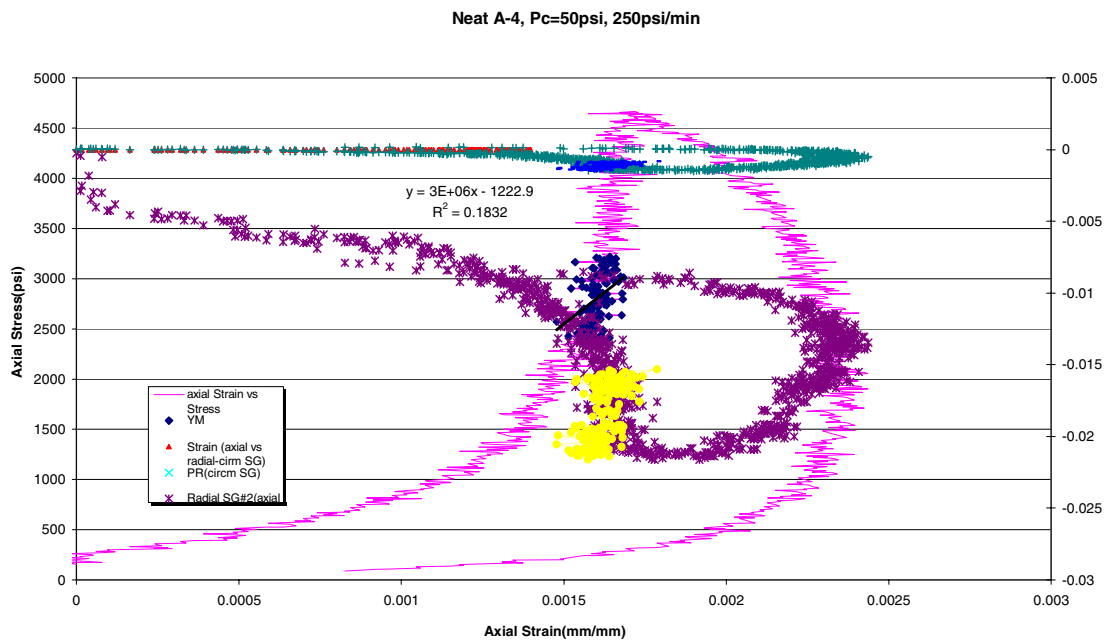
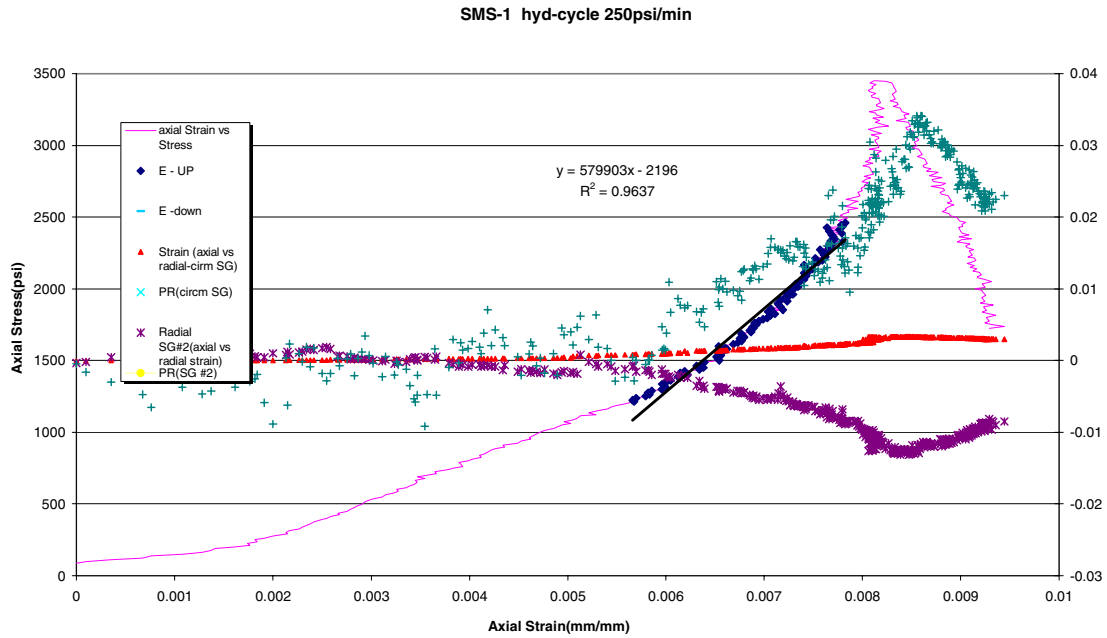




Figure B23— Hydrostatic cycling data for sodium metasilicate (SMS) slurry showing anelastic strain.





Appendix C—Numerical Modeling

The University of Houston has been contracted to perform finite element analysis (FEA) of the laboratory models used in the project (temperature and pressure cycling models).

Introduction

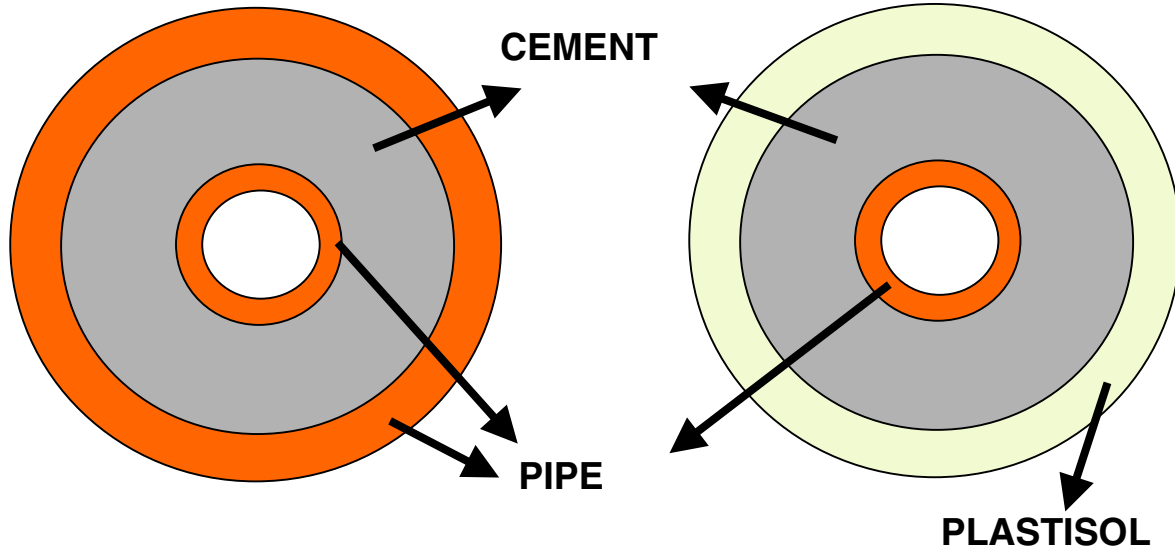
In understanding the long-term integrity of cement in deepwater systems and determining the properties that affect the ability of cement to seal fluids, a principal step is to mathematically model the system to study different stress-causing phenomena. Besides allowing a theoretical prediction of the effect of various stress conditions such as temperature cycling, pressure cycling etc., the models will also provide a means of justification to test the designs and steer the direction of laboratory testing. The results of these models will be analyzed to determine if the stresses associated with the stress-causing conditions will result in loss of annular seal of cement.

Further, in the presence of asymmetrical far-field stresses, internally pressurized and cemented wells can experience both tensile and compressive stresses. If the internal pressure is sufficiently high, fracture initiation can result. The cement's tensile strength and the tensile stresses induced within the cement sheath make some portions of the cement sheath particularly vulnerable to fracture initiation. The stress distribution in a casing-cement-rock system needs to be estimated as a single continuous problem over disjointed domains. It is presumed that a fundamental study of such systems will provide valuable clues that will aid in the selection of well completion techniques and appropriate cement properties.

Two main configurations have been considered for modeling purposes: hard formation and soft formation (**Figure C1**). The focus will be on establishing a mathematical framework for analyzing different loading conditions, temperature gradients, and material properties and their effect on the induced stress distribution. Long-term effects such as subsidence and compaction may also necessitate changes in loading conditions. A parametric variation of a cement's material properties and thickness has been studied to determine the role of each variable in determining the overall stress and strain distributions.



Figure C1—Hard formation and soft formation configurations



The following sections describe briefly the mathematical model and discuss the main results of the analysis.

Mathematical Model

In practice, the magnitude and orientation of the *in situ* stress field is altered locally by the drilling of a well. In addition, when internal wellbore pressure and temperature gradients are present, the pre-existing stress fields are distorted significantly, giving rise to new induced stresses. The following equation summarizes the regular elasticity problem, with internal wellbore pressure and far-field boundary conditions:

$$\begin{aligned}
 \nabla \cdot \sigma &= 0 && \text{on } B \\
 \varepsilon &= \frac{1}{2} (\nabla u + \nabla u^T) \\
 \sigma &= L \varepsilon \\
 e_i \cdot (\sigma \cdot n) &= \hat{\sigma}_1 && \text{on } \partial B_{li}
 \end{aligned} \tag{1}$$

where σ is the stress tensor
 ε is the strain tensor
 u is the displacement vector
 L is the elasticity tensor

The last equation represents the traction boundary condition specified on the internal and external boundaries.



In deepwater conditions, the subsea temperature will be lower ($< 5^{\circ}\text{C}$) than the surface temperature. However, after prolonged production, the pipelines can reach much higher temperatures (approximately 100°C). As a result, a temperature gradient is created across the annular cylinders (casing and cement sheath).

When the temperature rise in a homogeneous body is not uniform, different elements of the body tend to expand at different rates, and the requirement that the body remain continuous conflicts with the requirement that each element expand by an amount proportional to the local temperature rise. Thus, the various elements exert a restraining action upon each other that results in continuous unique displacements at every point. The system of strains produced by this restraining action cancels out all, or part of, the free thermal expansions at every point, ensuring continuity of displacement. This system of strains must be accompanied by a corresponding system of self-equilibrating stresses known as thermal stresses. A similar system of stresses may be induced in a structure made of dissimilar materials, even when the temperature change throughout the structure is uniform. Also, if the temperature change in a homogeneous body is uniform and external restraints limit the amount of expansion or contraction, the stresses produced in the body are termed thermal stresses.

In a completed wellbore system, all three conditions— nonuniform temperature distribution, dissimilar materials (casing, cement etc.), and external restraints— are present and contribute towards thermal stresses.

The desired energy equation for an isotropic, elastic solid is:

$$k\nabla^2 T = C_{e=0} \frac{\partial T}{\partial t} + \beta T_0 \frac{\partial e'}{\partial t} \quad (2)$$

where k is the thermal conductivity

T is the temperature rise from the initial uniform temperature T_0 , of the stress-free state

$\beta = E\alpha/(1-2\nu)$, $C_{e=0}$ is the heat capacity per unit volume at zero strain

e' is the dilatation

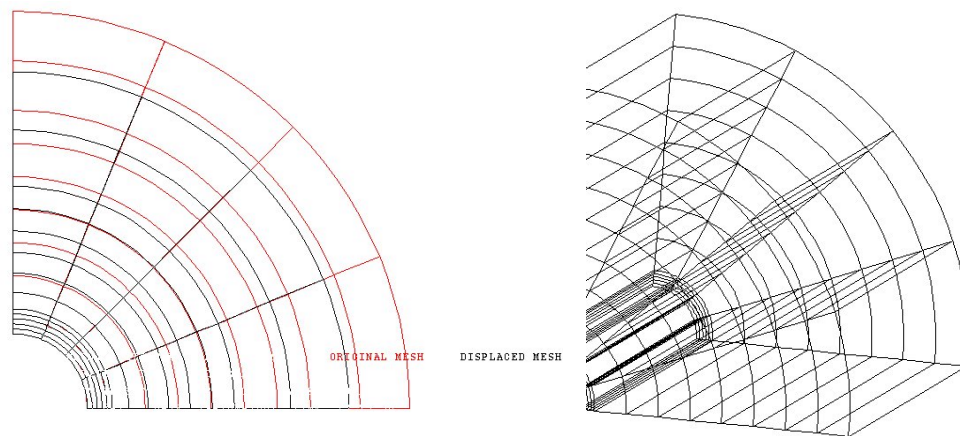
This equation, based on the Fourier law of heat condition and the linear thermoelastic stress-strain relations, shows that the temperature distribution in a body depends upon the dilatations throughout the body. Thus, the temperature and strain (stress) distributions are coupled and an exact analysis requires the simultaneous determination of the stress and temperature profiles.

For numerical modeling purposes, the casing-cement-rock system is considered to be concentric cylindrical structures in continuous contact with each other. The hard formation configuration represents a hard formation, while the soft formation configuration represents a soft formation. A generic, 3D finite element model is



developed for this composite system with Abaqus 5.7 and Matlab 6.0 (**Figure C2**). Pure elastic stress-strain analysis is performed with customized Matlab programs, while thermal stress analysis is performed with Abaqus. For laboratory tests involving homogeneous casing and confining pressures, the system is axi-symmetric and hence, only a quadrant of the annular structure is studied.

Figure C2—3D finite element model grid



Assumptions

The following assumptions are made in modeling a cement system:

- The system can be modeled on the basis of linear elastic theory.
- The composite system retains continuity at the interfaces.
- The system is axi-symmetric because of the boundary conditions.
- All materials are homogeneous and continuous.
- Plastisol has the same material properties as rubber.
- Plane stress condition is valid.

Stress Conditions

The following stress-causing conditions have been considered for mathematical modeling purposes:

- Normal production operation
- Pressure cycling (casing pressure)
- Subsidence, compaction (confining pressure)
- Temperature cycling (thermal stress)

The normal production operation includes an operating casing pressure and an external confining pressure (*in situ* stresses), along with a steady thermal gradient. All elastic and thermoelastic simulations represent steady-state conditions. A fully rigorous, coupled



thermoelastic equation is considered for numerical modeling purposes. However, the effect of dilatation is negligible when the system is allowed to evolve up to steady-state conditions.

Parametric Studies

The following parameters and cement properties have been varied to study their influence on stress distribution in the cement:

- Casing pressure (100 to 10,000 psi)
- Confining pressure (100 to 1000 psi)
- Temperature gradient (80 to 180°F)
- Young's modulus (1000 to 7000 psi)
- Poisson's ratio (0.15 to 0.45)
- Cement thickness (1 to 7 in.)

All numerical simulations are representative of laboratory testing conditions, with the parameter ranges provided by CSI from experimental results. All parametric studies are conducted with respect to the following reference case:

Parameter	Value
Casing pressure	500 psi
Confining pressure	500 psi
Young's modulus	5000 psi
Poisson's ratio	0.35
Cement thickness	1 in.
No thermal gradient	

Stress, displacement, and temperature profiles for both the soft and hard formation configurations are computed using a 3D finite element model with quadratic elements. **Figure C3** shows the first principal stress and horizontal displacement profiles for a representative case (hard formation) with an internal casing pressure of 500 psi and no confining pressure or thermal gradient. A Young's modulus of 5000 psi and a Poisson's ratio of 0.35 were used for the cement sheath. When the cement has a relatively high Young's modulus (3.05×10^7 psi), most of the stress variation is arrested within the inner pipe (made of steel). As a result, very little stress is transferred across to the cement sheath. The outer pipe experiences hardly any load in the absence of a direct confining pressure, as is evident from the negligible stresses and displacements.



Cement		Compressive Strength* (psi) *After 10 days	Tensile Strength (psi)	Shear Bond (psi)	
				PIP	PIS
Foam		3436	578	321	147
Latex		3630	504	432	237
Baseline		4035	673	519.6	203

Casing pressure. The casing pressure is varied from 100 to 10,000 psi for the hard formation configuration in the absence of confining pressure or a thermal gradient. The first principal stress and horizontal displacement along the x-axis is plotted in **Figure C4**. Clearly, the inner steel pipe limits the transfer of any load to the cement sheath because of its high Young's modulus. A sharp stress contrast is observed at the casing-cement interface, while the continuity requirement of displacement at the interface manifests itself as differing gradients in the two materials and reaches zero at the external boundary. Since the inner steel pipe is the dominant material in determining load distribution, the cement sheath is hardly affected.

The same result, though more pronounced, is observed for the stress distribution in the soft formation configuration (**Figure C5**) in the absence of confining pressure. However, larger displacements are observed in comparison to the hard formation case, suggesting that the cement sheath can move further from its set position and can potentially lose its annular seal in a soft formation.

Confining pressure. In addition to base casing pressure of 500 psi, a confining pressure is applied on the outside of the casing, ranging from 100 to 1000 psi. All other conditions are held constant as before. The stress profile (**Figure C6**) is similar to that of casing pressure only, since both the inner and outer pipes are assumed to be of the same material (steel). The cement sheath has a reduced and almost uniform stress distribution, while the steel pipes arrest most of the variation.

For the soft formation configuration, a confining pressure results in relatively large deformations in both the cement and the Plastisol layer. However, increasing the confining pressure from 100 to 1000 psi has little effect on the magnitude of displacement in all three materials (**Figure C7**).

Young's modulus and Poisson's ratio. The cement material properties (Young's modulus and Poisson's ratio) are varied to study their effect on stress distribution in the hard formation configuration. The Young's modulus is varied between 1000 and 7000 psi, and the Poisson's ratio is varied from 0.15 to 0.45. Because the steel pipe transfers



very little stress to the cement sheath, there is a negligible influence on the stress and strain distribution in the cement sheath (**Figures C8 and C9**).

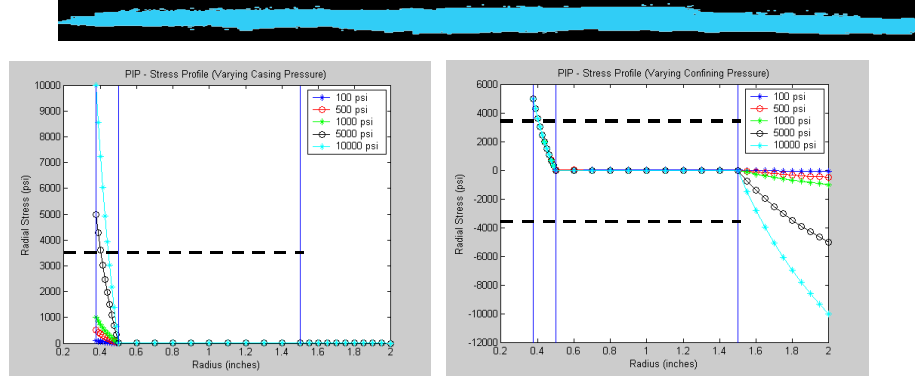
Cement thickness. The thickness of the cement layer is varied from 1 to 7 in. for the hard formation configuration. As the thickness increases, a larger portion of the cement is under compression, which increases horizontal displacement for the same casing and confining pressure, as shown in **Figure C10**. The same amount of net displacement is experienced by the inner and outer steel pipes, as compared with the more flexible cement sheath.

Temperature gradient. In addition to a casing pressure of 500 psi and a confining pressure of 500 psi, a thermal gradient is applied across the concentric cylinders for the hard formation configuration. The external temperature on the outer pipe is held constant at 68°F, and the temperature at the inner surface of the inner pipe is varied between 80°F and 180°F. The temperature profile is symmetric, and varies only along the radial direction (**Figure C11**). While the elastic stress acts in compression, the thermal stress arising due to nonuniform and dissimilar expansion of the composite system can lead to tensile stresses. As a result, the net stress experienced by the system is controlled by the dominant stress source. The displacement profile (**Figure C12**) indicates that the thermal stresses tend to expand the concentric cylinders. At high temperatures and low external loads, the thermal stress can control the net displacement, and vice-versa at low temperatures and high external loads.



Figure C3—

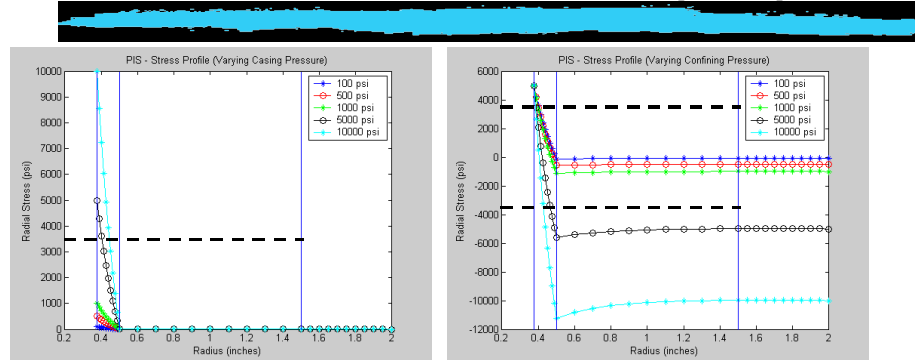
COMPRESSIVE FAILURE (PIP)



- Annular cement in PIP retains its integrity at high casing and confining pressures

Figure C4—

COMPRESSIVE FAILURE (PIS)



- Annular cement in PIS fails in compression at high confining pressures



Figure C5—

SHEAR FAILURE (PIP)



Casing Pressure

15 psi

Confining Pressure

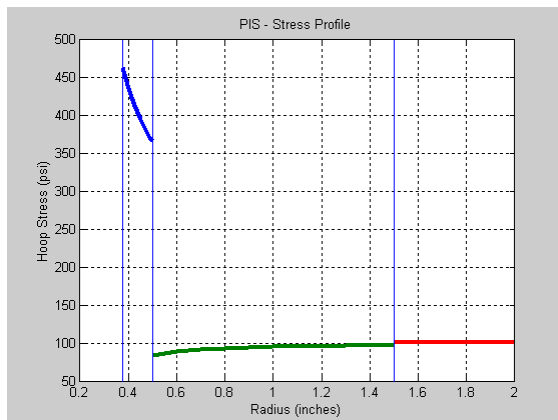
100 psi

Hoop Stress Contrast

~ 450 psi

Figure C3—

SHEAR FAILURE (PIS)



Casing Pressure

15 psi

Confining Pressure

100 psi

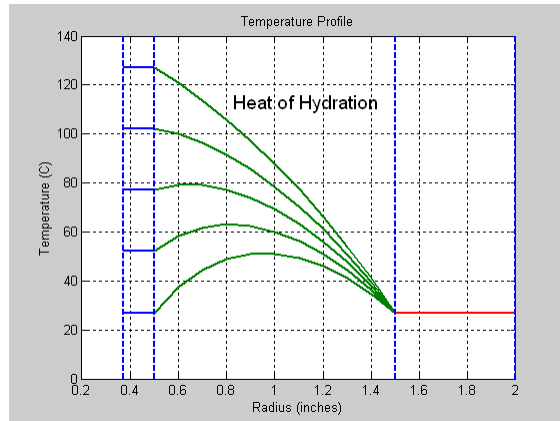
Hoop Stress Contrast

~ 300 psi



Figure C7—

HEAT OF HYDRATION

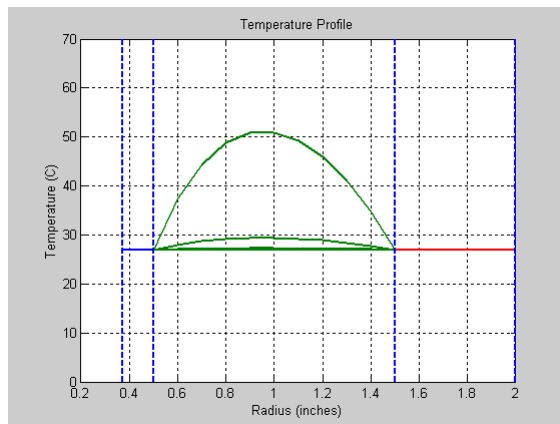


Borehole Temperature
300 K – 400 K

Heat of Hydration Rate
3.5 KJ/Kg.sec

Figure C8—

HEAT OF HYDRATION



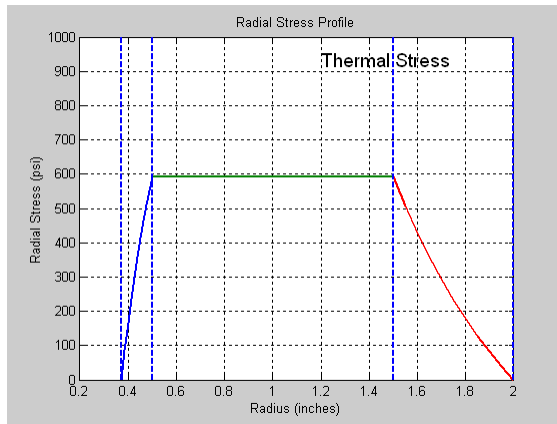
Borehole Temperature
300 K

Heat of Hydration Rate
3.5 J/Kg.sec - 3.5 KJ/Kg.sec



Figure C9—

HEAT OF HYDRATION



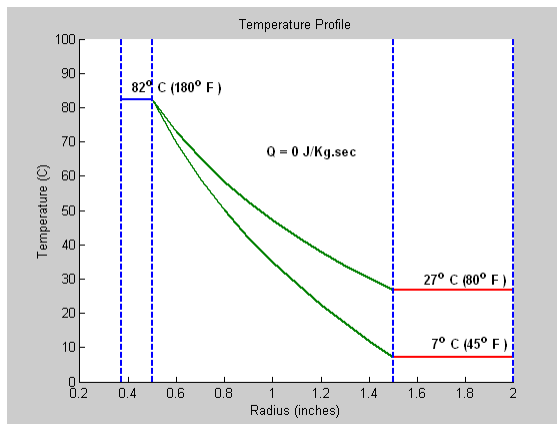
Borehole Temperature
300 K

Reservoir Temperature
300 K

Linear Superposition with
Elastic Stress

Figure C10—

THERMAL STRESS



Borehole Temperature
180° F

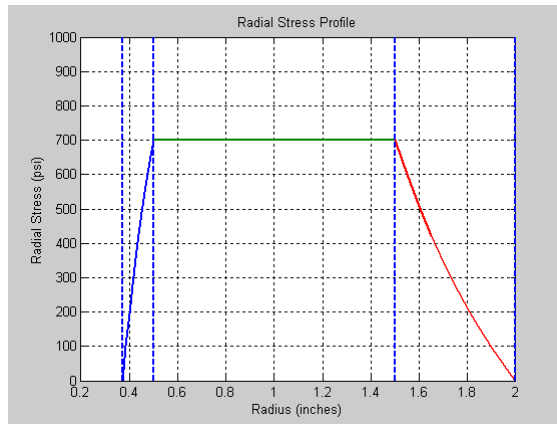
Reservoir Temperature
45° F, 80° F

Heat of Hydration Rate
0 J/Kg.sec



Figure C11—

THERMAL STRESS



Borehole Temperature
180° F

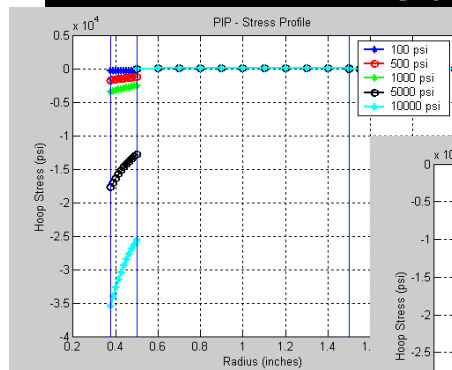
Reservoir Temperature
45° F, 80° F

Heat of Hydration Rate
0 J/Kg.sec

- Higher Thermal Stress
- No significant variation within Cement

Figure C12—

HOOP STRESS (TENSILE)



Confining Pressure
0 psi

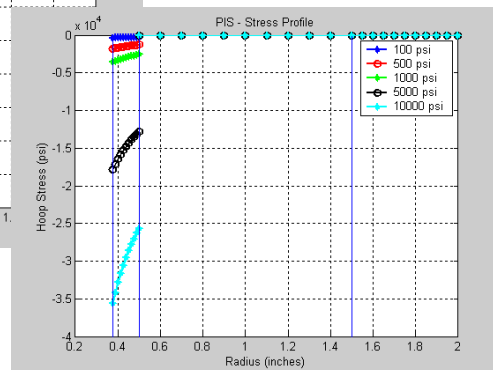


Figure C13—

DISPLACEMENT PROFILE

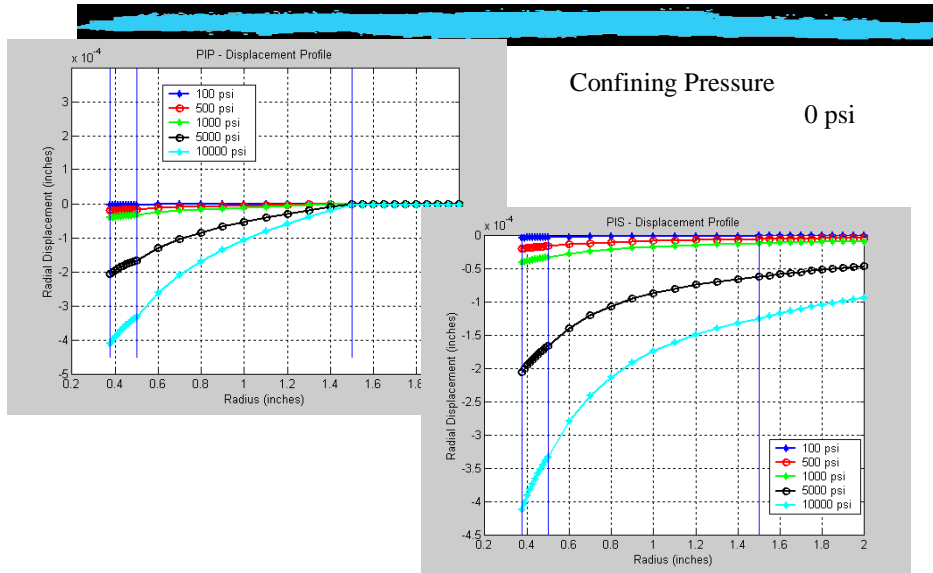


Figure C14—

HOOP STRESS (TENSILE)

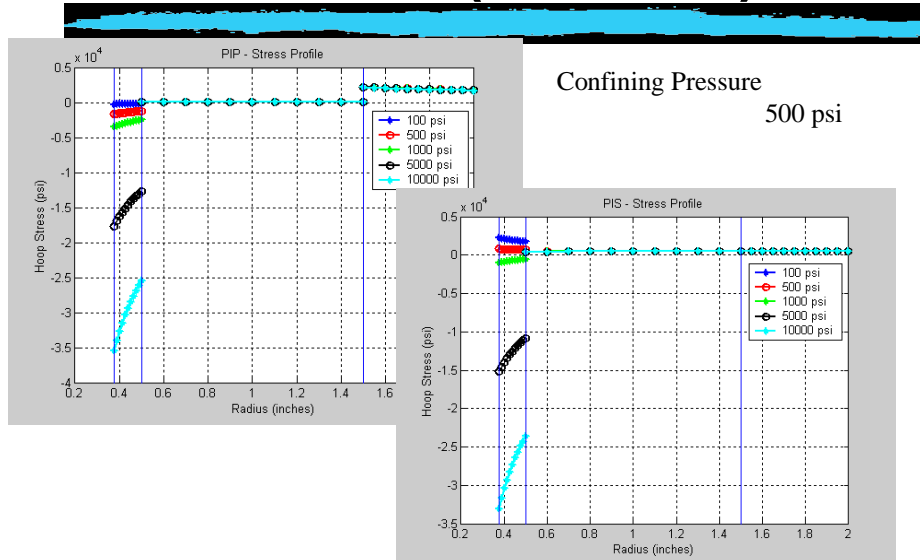
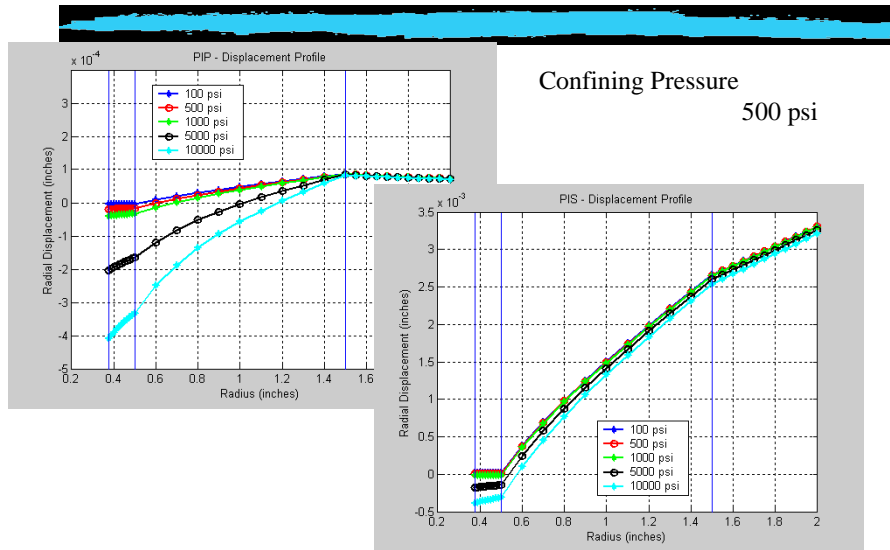




Figure C15—

DISPLACEMENT PROFILE



¹ API Spec. 10, 22nd Edition, American Petroleum Institute, Washington, D.C., December 1997.

² Standard Test Method for Static Modulus of Elasticity (Young's Modulus) and Poisson's Ratio of Concrete in Compression, ASTM C469-02, ASTM International, March 1, 2002.

³ "Standard Test Method for Splitting Tensile Strength of Cylindrical Concrete Specimens," ASTM C496-96, ASTM International, March 1, 1996.